

UNIVERSITY OF HAWAII LIBRARY

The Accuracy of Monitoring the Transports of the
Equatorial Currents in the Central Pacific Ocean

A thesis submitted to the Graduate Division of the
University of Hawaii in partial fulfillment
of the requirements for the degree of

Master of Science

in Oceanography

May, 1986

By

Wayne L. Tang

Thesis Committee:

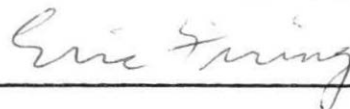
Klaus Wyrтки, Chairman
Eric Firing
Peter Muller

We certify that we have read this thesis and that, in our opinion, it is satisfactory in scope and quality as a thesis for the degree of Master of Science in Oceanography.

THESIS COMMITTEE



Chairman



Acknowledgements

I wish to express my deep appreciation to the chairman of my thesis committee, Prof. Klaus Wyrski, for his invaluable advise and and constructive criticism he has given me throughout the writing of this thesis. I also wish to thank Dr. Eric Firing and Dr. Peter Muller for their assistance.

I am very grateful to Shikiko Nakahara for her help in computer programming.

Abstract

Data from the Hawaii to Tahiti Shuttle Experiment was used to develop a scientific basis for monitoring the equatorial currents in the Pacific Ocean. Geostrophic transports relative to 300 and 1000 meters were calculated for each section of the Shuttle Experiment. Dynamic heights, steric heights, and isotherm depths were also determined at the ridges and troughs as well as measurements of sea level from several island stations.

Geostrophic transports were compared with estimates of transport from several indirect methods which only used data from the ridges and troughs. By examining the correlations and standard errors of estimation of these comparisons it is shown that the mass transports of the equatorial currents in the central Pacific Ocean can be accurately monitored by a variety of indirect methods during normal periods. It was found that isotherm measurements at the ridges and troughs provided a fairly accurate method of monitoring transports for the North Equatorial Counter Current and the North Equatorial Current while determining steric heights at the ridges and troughs provided the best monitoring method for the South Equatorial Current. In some cases, sea level can be used to monitor transports with a fair amount of accuracy. These simple methods provide an alternative to the more expensive conductivity-temperature depth sections.

Table of Contents

	Page
Acknowledgements	iii
Abstract	iv
List of Tables	vi
List of Illustrations	vii
List of Abbreviations	viii
I. Introduction	1
II. Data Acquisition and Location	5
III. Data Processing	6
IV. Method	14
V. Results and Discussion	16
A. Comparing Sea Level with Dynamic Heights, Steric Heights, Isotherm Depths, and Transport Estimates	16
B. Comparisons between Sea Level Differences and Transport Estimates for the SEC and UC	33
C. Comparisons between Dynamic Heights and Isotherm Depths at the Ridges and Troughs	36
D. Comparisons between Geostrophic Transports and Indirect Estimates of Transport	42
1. North Equatorial Counter Current	42
2. North Equatorial Current	44
3. South Equatorial Current	45
E. Comparisons between XBT and CTD Measurements 1/2 Degree Apart	50
F. Zonal Variability of the NECC	56
G. Sources of Error	58
VI. Conclusions	60
Appendix	
Figures 1 through 15	64
References	82

List of Tables

Table		Page
I	Comparisons with Sea Level near the following Ridges and Troughs:	
	A. North Equatorial Counter Current (Ridge)	24
	B. North Equatorial Current (Ridge)	26
	C. South Equatorial Current (Ridge)	28
	D. South Equatorial Current (Trough)	30
	E. Correlations among Sea Level Stations	32
II	Comparing Sea Level Differences with Transport Estimates for the SEC and UC	35
III	Comparisons between Dynamic Heights and Isotherm Depths at the Ridge and Trough of the:	
	A. North Equatorial Counter Current	39
	B. North Equatorial Current	40
	C. South Equatorial Current	41
IV	Comparisons between Geostrophic Transports and Indirect Estimates of Transport for the:	
	A. North Equatorial Counter Current	47
	B. North Equatorial Current	48
	C. South Equatorial Current	49
V	Comparisons Between XBT and CTD Measurements 1/2 Degree Apart	55
VI	Zonal Variability of the NECC	57
VII	The Accuracy of Estimating Geostrophic Transports relative to 300 and 1000 meters	63

List of Illustrations

Figure	Page
1 Location of the Shuttle Experiment	65
2 Time-latitude diagram of the Shuttle Experiment . .	66
3 Positions of the ridges and troughs during the Shuttle Experiment	67
4 Mean dynamic height and isotherm topography during the Shuttle Experiment	68
5 Fanning sea level vs. SH300 at the NECC ridge . . .	69
6 Fanning sea level vs. AXBT SH300 TX for the NECC . .	70
7 Christmas sea level vs. PCM transports for the NECC	71
8 Depth of the 14 degree isotherm in meters along 158 West	72
9a T-S relations between 20 North and 8 North during the Shuttle Experiment	73
9b T-S relations between 4 North and 4 South during the Shuttle Experiment	74
9c T-S relations between 8 South and 16 South during the Shuttle Experiment	75
10 Sea level differences between Papeete and Jarvis Island vs. Taft DH300 TX for the SEC	76
11 Sea level differences between Penrhyn and Jarvis Island vs. Undercurrent Transports along 158 West .	77
12 Comparisons between D20 and dynamic heights at the ridge and trough of the NECC	78
13 DH300 vs DH1000 for the SEC	79
14 2-Layer Approx. vs. Taft DH300 TX for the NECC . . .	80
15 DEL SH300 vs. TAFT DH300 TX for the SEC	81

List of Abbreviations

- AXBT - air-expendable bathythermograph
- CTD - conductivity-temperature-depth recorder
- D14 - depth of the 14 degree isotherm for the NEC or SEC
- D20 - depth of the 20 degree isotherm for the NECC
- D14 TROUGH - maximum depth of the 14 degree isotherm
below a sea level ridge for the NEC or SEC
- D14 RIDGE - minimum depth of the 14 degree isotherm
below a sea level trough for the NEC or SEC
- DEL D14 - difference in depth of the 14 degree isotherm
between the ridge and trough of the NEC or SEC
- D14BAR - average depth of the 14 degree isotherm
between the ridge and trough of the NEC or SEC
- DH300 - dynamic height relative to 300 meters
- DH1000 - dynamic height relative to 1000 meters
- DH300 TX - approx geostrophic transport relative to 300
meters from data taken at the ridge and trough
- DH1000 TX - approx geostrophic transport relative to 1000
meters from data taken at the ridge and trough
- DYN CM - dynamic centimeters (units of dynamic height)
- NEC - north equatorial current
- NECC - north equatorial counter current
- PCM - profiling current meter
- SEC - south equatorial current
- SH300 - steric height relative to 300 meters
- SH300 TX - approx geostrophic transport relative to 300
meters using a mean T-S relation at the
ridge and trough

ST CM - steric centimeters (units of steric height)

SV - sverdrups (1,000,000 cubic meters of water per second)

TAFT DH300 TX - geostrophic transport relative to 300
meters calculated from data taken at each
station between the ridge and trough

TAFT DH1000 TX - geostrophic transport relative to 1000
meters calculated from data taken at each
station between the ridge and trough

XBT - expendable bathythermograph

I. INTRODUCTION

The importance of ocean-atmosphere interaction and its role in short-term climatic fluctuations has made it desirable to monitor changes in the ocean environment. Current monitoring in particular has received much attention lately.

Besides its use as a tool in climate forecasting, ocean current monitoring may prove useful in research studies such as verifying ocean circulation models or estimating heat flux and storage due to advection. It may also prove useful in ocean navigation routing.

Another potentially important use is for the monitoring of El Nino. Oceanic circulation plays an important role in the formation of El Nino by altering the pattern of sea surface temperatures through advection (Meyers and Donguy, 1984). Previous El Nino events have been preceded by changes in the equatorial currents. By accurately monitoring these currents, one might then be able to predict an El Nino.

It has already been demonstrated that dynamic height, sea level, and the 2-Layer Approximation of geostrophic transport can be used to monitor low frequency variations of equatorial currents (Wyrтки, 1978). Ocean current monitoring from hydrographic sections and sea level stations

has also been carried out in the Antarctic Circumpolar Current (Whitworth, 1983) and the Florida Current (Molinari et al., 1985), however, little attention has been paid to how accurate these monitoring methods are. This is the main reason why I have chosen to evaluate the accuracy of different monitoring methods by examining data from the Hawaii to Tahiti Shuttle Experiment. My goal is to determine the most simple, accurate, and economical method of monitoring the equatorial currents.

The Hawaii to Tahiti Shuttle Experiment was conducted between January 1979 and June 1980. It was designed to observe the changing equatorial ocean structure and circulation (Wyrtki et al., 1981). By studying the variations and interactions of the four major equatorial ocean currents, a scientific method for their monitoring is developed based on simple observations of the thermal structure and sea level. This thesis will examine and determine the accuracy of different monitoring methods for each of the four equatorial currents:

- 1.) The North Equatorial Counter Current (NECC)
- 2.) The North Equatorial Current (NEC)
- 3.) The South Equatorial Current (SEC)
- 4.) The Undercurrent

The North Equatorial Counter Current (NECC)

The NECC is the most well defined of the four equatorial currents. It flows eastward between a sea level ridge near 10 North and a sea level trough near 4 North. The isotherm field is characterized by a very sharp temperature gradient with the 20 degree isotherm near the center. Transports vary from 0 SV to more than 50 SV with an average around 20 SV. Average speeds are about 20 cm/s.

The North Equatorial Current (NEC)

The NEC flows westward between about 10 North and 20 North. The 14 degree isotherm is located within the north-south sloping thermocline. The NEC is not a broad uniform flow but may be split into several branches and may contain eddies. Transports vary from roughly 10 SV to 30 SV with an average around 20 SV. Average speeds are about 10 cm/s.

The South Equatorial Current (SEC)

The SEC is split into a northern portion between the NECC ridge and the SEC trough near the equator and a southern portion between the SEC trough and the SEC ridge near 10 South. Near the equator it is swift and shallow, flowing westward above the Undercurrent. South of the equator the thermocline spreads as its isotherms slope

toward the south. This is best represented by the 14 degree isotherm. Transport in this portion of the SEC varies from roughly 20 to 50 SV with an average around 30 SV. Average speeds are about 15 cm/s.

The Undercurrent

The Undercurrent flows eastward along the equator and is characterized by a spreading of the isotherms. Its core is located between 100 and 200 meters depth and sometimes meanders about the equator. Transports vary from 0 to more than 80 SV with an average around 30 SV. Average speeds are about 30 to 40 cm/s with core speeds around 80-100 cm/s.

II. DATA ACQUISITION AND LOCATION

During the Hawaii to Tahiti Shuttle Experiment, there were 14 transequatorial cruises, approximately one per month between February 1979 and June 1980, resulting in 44 XBT and CTD sections across the equatorial Pacific Ocean. In addition, AXBT sections were made twice per month during this period resulting in 35 additional sections (see fig. 1 and 2). Each transequatorial cruise included three meridional sections:

- 1) 158 West longitude between 21N and 4S
- 2) 153 West longitude between 4S and 12N
- 3) 150 West longitude between 12N and 17S

In this manner, maximum coverage of the NECC, the Undercurrent, and the northern portion of the SEC was obtained.

During each cruise, CTD stations to 1000 meters were taken at one degree latitude intervals, supplemented by intermediate XBT observations to 400 meters or more. In addition to these profiles, temperature sections were obtained to depths greater than 300 meters by AXBT's along the same three meridians but at different times. It is from these three instruments (CTD, XBT, and AXBT) that the monitoring methods derive their data.

III. DATA PROCESSING

The CTD profiles, digitized at depth intervals of 10 meters, were used to compute density. Dynamic heights were then calculated by integrating the density anomaly from the surface to reference depths of 300 and 1000 meters (Wyrтки and Kilonsky, 1982)

Steric heights relative to 300 meters were similarly calculated from XBT's and AXBT's using salinity from a mean T-S relation (steric heights are dynamic heights calculated from a mean T-S relation). This mean T-S relation was determined from a one-year period starting from April 1979 and ending in March 1980. Because the first and last cruise were not complete and because winds started to weaken and temperatures started to rise near the end of the shuttle Period, this chosen period was the least disturbed one-year segment during the Shuttle Experiment.

The locations of the ridges and troughs were then determined as the latitudes with the highest and lowest values of steric and dynamic height. Figure 3 shows a time series of the locations of the ridges and troughs as determined from the steric and dynamic height topography relative to 300 meters. The locations of the ridges and troughs vary seasonally and interannually, however, the range of variation is confined to a fairly narrow band. The

ridges and troughs can therefore be located rather easily by sampling at a few discrete points. In some cases, the ridges and troughs were relatively flat making their exact locations difficult to determine, but in general, sampling at one degree latitude intervals over several degrees is enough to resolve their positions. This type of discrete sampling can take place on ships of opportunity or near strategically located islands. Satellite altimetry could also aid in determining the locations of the ridges and troughs. This would greatly benefit indirect methods of estimating transport that rely only on measurements at the ridges and troughs.

This thesis exploits the fact that the locations of the ridges and troughs can be determined rather easily. There are several methods of monitoring transports which rely only on measurements at the ridges and troughs. These methods are now described and later it will be shown how well their estimates correlated with standard calculations of geostrophic transports.

a.) Dynamic and Steric Height Differences:

After the locations of the ridges and troughs were determined, dynamic and steric height differences between

the ridges and troughs were calculated relative to 300 and 1000 meters. These differences give estimates of sea level slope and surface current strength:

$$\text{DEL DH300} = \text{DH300 RIDGE} - \text{DH300 TROUGH}$$

$$\text{DEL SH300} = \text{SH300 RIDGE} - \text{SH300 TROUGH}$$

$$\text{DEL DH1000} = \text{DH1000 RIDGE} - \text{DH1000 TROUGH}$$

b.) Approximate Geostrophic Transports:

Approximate geostrophic transports (CTD DH300 TX and CTD DH1000 TX) is another estimate of transport which relies on measurements taken only at the ridges and troughs. CTD DH300 TX and CTD DH1000 TX were calculated by integrating the density anomaly from the surface to reference depths of 300 and 1000 meters at the ridge and trough and then taking the difference between the two:

$$\text{CTD DH300 TX} = \left(\frac{gL}{f} \right) \times \left[\int_0^{300} (\alpha \text{ at ridge}) dz - \int_0^{300} (\alpha \text{ at trough}) dz \right]$$

$$\text{CTD DH1000 TX} = \left(\frac{gL}{f} \right) \times \left[\int_0^{1000} (\alpha \text{ at ridge}) dz - \int_0^{1000} (\alpha \text{ at trough}) dz \right]$$

where g = acceleration of gravity
 L = width of the current (assumed constant)
 α = density anomaly
 f = coriolis parameter for latitude midway
between the ridge and trough

It was later found that correlations for comparisons between approximate geostrophic transports and other indirect estimates were significantly better if the Coriolis Parameter f was assumed to be constant. Correlations between two independent measures of the thermal structure is lower if the Coriolis parameter f , which introduces a latitudinal dependency, is utilized in only one of the measures, therefore f was assumed to be constant for calculations of approximate geostrophic transports. The constant f was chosen corresponding to the latitude midway between the ridge and trough, i.e. 14 North for the NEC, 7 North for the NECC, and 5 South for the SEC.

c.) Isotherm Depth Differences:

Another estimate of transport comes from isotherm depth differences. The 20 degree isotherm depth (D20) for the NECC and the 14 degree isotherm depth (D14) for the NEC and SEC were obtained at the ridges and troughs. These isotherms were chosen because they most closely represent the thermocline and its variations. The difference between the maximum isotherm depth at the D20 or D14 trough and the minimum isotherm depth at the D20 or D14 ridge was then used as an estimate of transport:

$$\begin{aligned} \text{DEL D20} &= \text{maximum difference of D20 for the NECC} \\ &= \text{D20 TROUGH} - \text{D20 RIDGE} \end{aligned}$$

$$\begin{aligned} \text{DEL D14} &= \text{maximum difference of D14 for NEC or SEC} \\ &= \text{D14 TROUGH} - \text{D14 RIDGE} \end{aligned}$$

In general, the locations of the isotherm ridges coincide with the locations of the dynamic height troughs and the locations of the isotherm troughs coincide with the locations of the dynamic height ridges.

d.) 2-Layer Approximation Method:

From the two extreme isotherm depths, the 2-Layer Approximation of transport can also be derived based on the density structure of the current. Following Wyrski and Kendall (1967), one only needs to determine the isotherm depths at the ridge and trough of the current and the density contrast between the upper and lower layer to estimate the transport according to the following equation:

$$\begin{aligned} \text{2-Layer approx. of transport} &= \frac{g}{f} \times \frac{\text{del } \rho}{\rho} \times \frac{1}{2} (D20T - D20R) (D20T + D20R) \\ &= \frac{g}{f} \times \frac{\text{del } \rho}{\rho} \times \text{DEL D20} \times \text{D20BAR} \end{aligned}$$

where del ρ = difference in density between the two layers
 D20T = depth of the 20 degree isotherm at the trough
 D20R = depth of the 20 degree isotherm at the ridge
 D20BAR = average depth of the 20 degree isotherm

In a manner similar to the approximate geostrophic transport computations, I assumed that the Coriolis Parameter f , density ρ , and del ρ were constant. Therefore, DEL D20 x D20BAR is used as an estimate of transport for the NECC and DEL D14 x D14BAR is used as an estimate of transport for the NEC and SEC.

In summary, estimates of the strength of the equatorial currents are derived from 4 different monitoring methods:

- a.) Dynamic and Steric Height Differences relative to 300 and 1000 meters between the ridge and trough (DEL SH300, DEL DH300, and DEL DH1000)
- b.) Approximate Geostrophic Transport Method (CTD DH300 TX and CTD DH1000 TX)
- c.) Differences in depth of the 20 and 14 degree isotherm between the ridge and trough (DEL D20 and DEL D14)
- d.) The 2-Layer Approximation Method (DEL D20 x D20BAR and DEL D14 x D14BAR)

All of these methods involve calculating or measuring parameters (dynamic heights, steric heights, and isotherm depths) at only two points, the ridge and trough, whose location can be determined from satellite altimetry, ships of opportunity, or from strategic sampling near islands.

Three additional estimates of transport were obtained from independent sources:

1.) Profiling Current Meter (PCM)

Profiling current meters (PCM) were used to make direct measurements of the flow field from the surface to 500 meters at each degree of latitude between 10 North and 4 South. In all, there were 41 sections that crossed the equator. Direct transports of the NECC, SEC (between 3 North and 3 South), and Undercurrent were calculated by vertically integrating velocities greater than

10 cm/s from the surface to 300 meters (Firing, 1981). There are several errors associated with these direct measurements of transport and they are discussed later on page 58.

2.) Sea Level Differences

Several islands in the central Pacific are strategically located near the ridges and troughs of dynamic height and isotherms. Figure 4 shows the close proximity of these islands to the ridges and troughs. The Hawaiian islands (20 North) are located near the NEC ridge, Fanning (4 North) is located near the NECC ridge, Jarvis (0 South) is located near the SEC trough, and Penrhyn (9 South) and Papeete (18 South) are located near the SEC ridge. One can therefore estimate sea level slope across a current by measuring sea level differences between two islands located near the ridge and trough of that current. For example, the sea level slope across the SEC can be estimated well from sea level differences between Penrhyn and Jarvis. This sea level difference is used as an estimate of transport for the SEC. A 7-day running average of sea level was used for all comparisons with sea level. Unfortunately, there are no islands near the NECC trough so the sea level slope across the NEC and NECC cannot be measured.

3. Geostrophic Method

Geostrophic transports were calculated for the NECC, NEC, and SEC from data taken at each station between the ridge and trough. The most comprehensive calculations of geostrophic transport are provided by Taft (1981). Taft first contoured the salinity and temperature data with a linear interpolation Program. Salinity data were smoothed a second time with a 5-point binomial running average. Geostrophic transports relative to 300 and 1000 meters (TAFT DH300 TX and TAFT DH1000 TX) were then calculated between stations one degree of latitude apart after a 3-point binomial filter was applied to the dynamic heights. All zonal components less than 5 cm/s in magnitude were excluded from the integration.

IV. METHOD

In general, the geostrophic method estimates current transport as well as any other method including direct measurements of the flow field. Montgomery and Stroup (1962) have demonstrated through careful analysis of current observations and hydrographic data that the geostrophic approximation is valid even in very low latitudes.

Taft calculated geostrophic transports relative to 300 and 1000 meters for each current during the Shuttle Experiment. His calculations of geostrophic transports are used as the standard with which all other estimates of transport are compared. I compared TAFT DH300 TX and TAFT DH1000 TX with indirect estimates of current transport (discussed previously) which are based only on measurements at or near the ridges and troughs: Dynamic and Steric Height Differences, Approximate Geostrophic Transports, Isotherm Differences, 2-Layer Approximation Method, and Sea Level Differences. These indirect estimates of transport were also compared with direct estimates of transport from the PCM though more confidence is placed on Taft's values than on the PCM values.

The correlations and standard errors of estimation for these comparisons then give some measure of how accurate different monitoring methods are in estimating geostrophic and direct transports. It is shown that transports can be

accurately and economically monitored by discriminantly sampling at a few discrete points near the ridges and troughs.

Besides determining the most accurate method of monitoring geostrophic transports for each current, the relationships among steric heights, dynamic heights, isotherm depths, and sea level were examined at the ridges and troughs. Sea level stations near the ridges and troughs were used to approximate sea level at the ridges and troughs. The correlations among these different parameters at the topographic highs and lows give an indication of how they are interrelated and what physical processes are responsible for their relationship. These relationships can also give us some insight into the physics of the thermal structure and dynamics of the circulation.

Comparisons were also made between values obtained by XBT's and CTD's at the ridges and troughs. Steric heights and isotherm depths from XBT's were compared with dynamic heights and isotherm depths from CTD's. The correlations and standard errors for these comparisons are used as a measure of how accurate XBT's estimate dynamic heights and isotherm depths at the ridges and troughs. Comparisons between XBT and CTD values cannot be strictly made since XBT and CTD profiles were alternately sampled at 1/2 degree intervals, however, good results were still obtained.

V. RESULTS AND DISCUSSION

A. COMPARING SEA LEVEL WITH DYNAMIC HEIGHTS, STERIC HEIGHTS, ISOTHERM DEPTHS, AND TRANSPORT ESTIMATES

Tables Ia-Ie show results of comparisons between sea level (7-day running average) and 6 different parameters of the equatorial currents:

- 1.) Steric and Dynamic Height relative to 300 and 1000 meters at the ridges and troughs (SH300, DH300 and DH1000)
- 2.) Isotherm Depths at the ridges and troughs
20 degree isotherm for the NECC (D20)
14 degree isotherm for the NEC and SEC (D14)
- 3.) Approximate Geostrophic Transports relative to 300 and 1000 meters (CTD DH300 TX and CTD DH1000 TX)
- 4.) Geostrophic Transports relative to 1000 meters (TAFT DH300 TX and TAFT DH1000 TX)
- 5.) PCM Measurements for the NECC and SEC
- 6.) Sea Level at nearby island stations

Comparisons with Sea Level for the NECC Ridge

Sea level at Fanning (4N,159W) and Christmas (2N,157W) were compared with dynamic and steric heights at the NECC ridge (Table IA). Fanning, located closer to the NECC ridge at 4 North, gave a significantly higher correlation (at the 90% confidence level) than Christmas for most comparisons with steric and dynamic height at the NECC ridge. Fanning sea level correlated the best with AXBT SH300 at the NECC ridge along 158 West with $R=0.94+$ and a standard error of

+ significant at the 0.1% level

+/- 2.2 steric cm (see fig. 5). Comparing Fanning sea level with CTD DH300 and CTD DH1000 ridge gave lower correlations of $R=0.77^*$ and $R=0.86^+$ respectively. This may be due to statistical fluctuations.

Fanning and Christmas sea level was also compared with D20 trough for the NECC. The results show that Fanning sea level correlated better with AXBT D20 trough ($R=0.89^+$) than with CTD D20 trough ($R=0.46$) along 158 West. This is probably due to a more favorable sampling period during the AXBT flights.

One surprising find was that sea level at Fanning, Christmas, and Jarvis correlated well with approximate geostrophic transports for the NECC. The strength of the NECC is proportional to sea level at the NECC ridge, consequently, sea level at Fanning, located near the NECC ridge, correlated well with approximate geostrophic transports. Christmas and Jarvis sea level also correlated well with estimates of transport for the NECC because sea level at Christmas and Jarvis behave similarly to sea level at Fanning (see Table Ie). Comparing Fanning sea level with AXBT SH300 TX across 158 West gave the highest correlation of $R=0.94^+$ and a standard error of +/- 2.7 SV (see fig. 6). Correlations were lower when comparing Fanning sea level with approximate geostrophic transports calculated from XBT's and CTD's (XBT SH300 TX and CTD DH300 TX).

* significant at the 1% level

Sea level at Fanning, Christmas, and Jarvis correlated well with TAFT DH300 TX and TAFT DH1000 TX for the NECC. The results show that geostrophic transport relative to 1000 meters (TAFT DH1000 TX) can be monitored during non-El Nino years with an accuracy of about 5 to 6 SV by measuring sea level at Jarvis, Fanning, or Christmas.

Comparing sea level with direct measurements of transport by the PCM along 150W, 153W, and 158W resulted in correlations of $R=0.51^*$ and a standard error of ± 8.5 SV at Fanning to $R=0.70+$ and a standard error of ± 7.3 SV at Christmas (see fig. 7).

The rather high correlations found between sea level and estimates of transport suggests that the NECC is zonally coherent and can be monitored fairly well from simple measurements of sea level.

Unfortunately, there are no island stations situated near the NECC trough located around 10 North.

Comparisons with Sea Level for the NEC Ridge

Sea level at Hilo, Honolulu, and Johnston were compared with dynamic and steric heights at the NEC ridge (Table Ib). Sea level again correlated significantly better (at the 90% confidence level) with AXBT measurements than with XBT or CTD measurements. This may be due to aliasing during the shuttle cruises by the ship when the XBT and CTD sections

were made. Aliasing includes errors due to sampling at times when non-periodic events such as eddies disrupt the thermal structure.

Honolulu sea level correlated well with AXBT SH300 ridge ($R=0.82+$) and correlated fairly well with AXBT D14 trough ($R=0.67$) for the NEC along 158 West. In contrast, the correlation was low when comparing Honolulu sea level with CTD DH300 ridge ($R=0.03$) and CTD D14 trough ($R=0.03$) for the NEC along 158 West. This can be attributed to aliasing during the shuttle cruises when several eddies drifted westward with the NEC (Wyrтки, 1982). During the shuttle cruises by the ship, 7 eddies were crossed near the NEC ridge while only 2 were crossed during AXBT flights along 158 West (see fig. 8). This would explain why AXBT measurements gave better results. Though these eddies near the NEC ridge may pose a problem in monitoring the NEC, the eddies located near the center of the current represent no real problem for monitoring the strength of the NEC.

Honolulu and Johnston sea level correlated well with AXBT SH300 TX along 158 West with $R=0.84+$ and a standard error of ± 2.3 SV, however, correlations were much lower when comparing Honolulu and Johnston sea level with other estimates of transport based on data from the shuttle cruises. This is again due to more favorable sampling

during the AXBT flights when there were relatively few eddies near the NEC ridge.

Correlations for comparisons with Hilo sea level were generally lower. This is probably due to the location of Hilo on the windward side of the Big Island of Hawaii which separates Hilo from measurements along 158 West.

Comparisons with Sea Level for the SEC Ridge

Sea level at Papeete and Penrhyn were compared with dynamic and steric heights at the SEC ridge (Table Ic). Sea level at Penrhyn correlated with AXBT SH300 ridge along 158 West very well with a correlation of $R=0.93+$ and a standard error of ± 1.2 steric cm. This is because Penrhyn is close to the SEC ridge located near 10 South. The correlation between Penrhyn sea level and AXBT SH300 ridge along 150W, 153W, and 158W was also high ($R=0.81+$) suggesting zonal coherence of the SEC ridge between 150 West and 158 West, however, comparing Papeete and Penrhyn sea level with XBT SH300 ridge and CTD DH300 ridge along 150 West resulted in low correlations. This may be due to the large distance between the measurements and to aliasing.

Comparing Papeete and Penrhyn sea level with CTD D14 trough for the SEC gave very low correlations. This is because the D14 trough may occasionally be located south of Papeete (see fig. 4).

Sea level at Papeete correlated well with CTD DH300 TX along 150 West with $R=0.77^*$ and a standard error of ± 4.9 SV while comparing Papeete sea level with TAFT DH300 TX gave a slightly lower correlation of $R=0.70^*$ and a standard error of ± 7.6 SV. The correlation was even lower when comparing Papeete sea level with TAFT DH1000 TX ($R=0.53$). CTD measurements were only taken along 150 West which accounts for the lower correlation at Penrhyn located along 158 West.

----- Comparisons with Sea Level for the SEC Trough -----

Jarvis (0 South, 160 West) is the only island near the SEC trough. Jarvis sea level, which can be affected by fluctuations of the surface current (Roemmich, 1984), correlated well with CTD DH300 and CTD DH1000 trough for the SEC along 150 West with $R=0.82^+$ (Table Id). Jarvis sea level also correlated well with XBT SH300 trough ($R=0.85^+$) for the SEC along 150 West even though the T-S relation is relatively unstable near the equator. In Figure 9b, the T-S relation at one degree north is quite variable due to water from the north mixing with water from the south in the region of the Undercurrent, however, this seems to have little effect on estimating sea level at the SEC trough with XBT's.

Jarvis sea level correlated well with CTD D14 ridge ($R=0.82+$) for the SEC along 150 West indicating a strong zonal coherence of the SEC trough between 150 West and 160 West.

Jarvis sea level correlated well with CTD DH300 TX ($R=-0.77*$) but not as well with TAFT DH300 TX ($R=-0.68*$) and TAFT DH1000 TX ($R=-0.60$) for the SEC along 150 West.

Jarvis sea level was also compared with PCM measurements for the SEC but the correlations were poor.

Comparisons were also made with Malden sea level but these correlations are lower than those found for comparisons with Jarvis sea level. This is because Jarvis island is closer to the SEC trough near the equator.

Sea Level Comparisons

Sea level (7-day running mean) at two island stations close to one another were compared with each other to obtain a measure of the degree of variability of sea level (Table Ie). Sea level comparisons were made only when a section was made. Sea level at Jarvis correlated well with sea level at Malden, Christmas, and Fanning. This indicates that sea level behaves in a uniform manner within a few degrees of the equator for time scales of one week and longer. Table Ie also shows that sea level at the islands near the equator is negatively correlated with sea level at

Papeete near the SEC ridge. This indicates that sea level at the SEC ridge and SEC trough behave in an opposite manner as if there was a pivot in the middle of the SEC.

Sea level at Honolulu, Hilo, and Johnston correlated well with each other, especially during the AXBT flights along 158 West when there were few eddies. This indicates that sea level near the NEC ridge also behaves in a uniform manner.

TABLE IA
COMPARISONS WITH SEA LEVEL NEAR THE NECC RIDGE

		(4N, 159W) FANNING SEA LEVEL			(2N, 158W) CHRISTMAS SEA LEVEL			
		CORRE- LATION	STD ERROR	No OF POINTS	CORRE- LATION	STD ERROR	No OF POINTS	
1.)	AXBT SH300 RIDGE	158W	0.94 ⁺	2.2 st cm	10	0.73 [*]	4.1 st cm	11
		ALL LONGITUDES	0.84 ⁺	3.1 st cm	30	0.67 ⁺	4.1 st cm	27
	XBT SH300 RIDGE	158W	0.76 [*]	3.7 st cm	13	0.65	4.3 st cm	10
		ALL LONGITUDES	0.72 ⁺	4.4 st cm	39	0.53 [*]	6.0 st cm	32
CTD DH300 RIDGE	158W	0.77 [*]	3.0 dyn cm	13	0.55	4.0 dyn cm	10	
	ALL LONGITUDES	0.73 ⁺	4.5 dyn cm	39	0.64 ⁺	5.3 dyn cm	32	
CTD DH1000 RIDGE	158W	0.86 ⁺	2.9 dyn cm	13	0.68	4.0 dyn cm	10	
	ALL LONGITUDES	0.79 ⁺	4.6 dyn cm	39	0.71 ⁺	5.5 dyn cm	32	
2.)	CTD D20 TROUGH	158W	0.46	13 m	13	0.48	11 m	10
		ALL LONGITUDES	0.65 ⁺	16 m	39	0.60 ⁺	17 m	32
	AXBT D20 TROUGH	158W	0.89 ⁺	8 m	9	0.72	13 m	9
ALL LONGITUDES		0.73 ⁺	12 m	30	0.52 [*]	16 m	27	

⁺ Significant at the 0.1 % level

^{*} Significant at the 1 % level

TABLE IA. (CONTINUED) COMPARISONS WITH SEA LEVEL NEAR THE NECC RIDGE

		(4N, 159W) FANNING SEA LEVEL			(2N, 158W) CHRISTMAS SEA LEVEL			(0S, 160W) JARVIS SEA LEVEL			
		CORRE- LATION	STD ERROR	No OF POINTS	CORRE- LATION	STD ERROR	No OF POINTS	CORRE- LATION	STD ERROR	No OF POINTS	
3.)	AXBT	158W	0.94 ⁺	2.7 sv	10	0.77 [*]	4.9 sv	10	0.70	5.5 sv	11
	SH300 TX	ALL LONG.	0.80 ⁺	4.2 sv	28	0.63 [*]	5.1 sv	24	0.65 ⁺	5.4 sv	30
	XBT	158W	0.80 [*]	5.0 sv	11	0.59 [*]	5.2 sv	8	0.72 [*]	5.7 sv	12
	SH300 TX	ALL LONG.	0.67 ⁺	6.0 sv	36	0.50 [*]	7.4 sv	29	0.62 ⁺	6.3 sv	36
4.)	CTD	158W	0.83 ⁺	3.4 sv	13	0.74 ⁺	3.0 sv	10	0.67 [*]	4.5 sv	14
	DH300 TX	ALL LONG.	0.74 ⁺	5.0 sv	39	0.71 ⁺	5.5 sv	30	0.71 ⁺	5.0 sv	38
	CTD	158W	0.75 [*]	6.3 sv	12	0.72 ⁺	4.6 sv	9	0.66	7.2 sv	13
	DH1000 TX	ALL LONG.	0.80 ⁺	6.3 sv	38	0.73 ⁺	7.3 sv	31	0.73 ⁺	7.3 sv	38
5.)	TAFT	158W	0.75 [*]	4.6 sv	13	0.76 [*]	3.7 sv	10	0.76 [*]	4.4 sv	14
	DH300 TX	ALL LONG.	0.77 ⁺	4.6 sv	39	0.75 ⁺	4.9 sv	32	0.76 ⁺	4.5 sv	40
	TAFT	158W	0.74 [*]	6.4 sv	13	0.81 ⁺	4.9 sv	10	0.81 ⁺	5.3 sv	14
	DH1000 TX	ALL LONG.	0.77 ⁺	6.1 sv	39	0.79 ⁺	6.1 sv	32	0.80 ⁺	5.5 sv	40
5.)	PCM	158W	0.31 [*]	7.5 sv	11	0.64 ⁺	4.7 sv	8	0.70	5.0 sv	11
		ALL LONG.	0.51 [*]	8.5 sv	33	0.70 ⁺	7.3 sv	24	0.66 ⁺	7.1 sv	33

⁺ Significant at the 0.1 % level

^{*} Significant at the 1 % level

TABLE IB

COMPARISONS WITH SEA LEVEL NEAR THE NEC RIDGE

	(20N, 155W) HILO SEA LEVEL			(21N, 158W) HONOLULU SEA LEVEL			(17N, 170W) JOHNSTON SEA LEVEL		
	CORRE- LATION	STD ERROR	No OF POINTS	CORRE- LATION	STD ERROR	No OF POINTS	CORRE- LATION	STD ERROR	No OF POINTS
1) AXBT SH300 RIDGE	0.67	5.5 st cm	12	0.82 ⁺	4.1 st cm	12	0.80 [*]	4.3 st cm	12
XBT SH300 RIDGE	0.12	5.2 st cm	14	-0.12	5.2 st cm	14	0.32	4.6 st cm	14
CTD DH300 RIDGE	0.19	4.1 dyn cm	14	0.03	4.4 dyn cm	14	0.27	3.9 dyn cm	14
CTD DH1000 RIDGE	0.23	5.5 dyn cm	14	0.03	6.2 dyn cm	14	0.14	5.8 dyn cm	14
2) AXBT D14 TROUGH	0.67	15 m	12	0.67	15 m	12	0.64	16 m	12
CTD D14 TROUGH	0.05	20 m	14	0.03	20 m	14	0.16	18 m	14

⁺ Significant at the 0.1 % level

^{*} Significant at the 1 % level

TABLE IB. (CONTINUED) COMPARISONS WITH SEA LEVEL NEAR THE NEC RIDGE

	(20N, 155W) HILO SEA LEVEL			(21N, 158W) HONOLULU SEA LEVEL			(17N, 170W) JOHNSTON SEA LEVEL		
	CORRE- LATION	STD ERROR	No OF POINTS	CORRE- LATION	STD ERROR	No OF POINTS	CORRE- LATION	STD ERROR	No OF POINTS
3) AXBT SH300 TX	0.69	3.2 sv	12	0.84 ⁺	2.3 sv	12	0.80 [*]	2.6 sv	12
XBT SH300 TX	0.09	3.4 sv	13	-0.06	3.4 sv	13	0.45	2.6 sv	13
CTD DH300 TX	0.16	2.4 sv	13	0.06	2.5 sv	13	0.50	1.8 sv	13
CTD DH1000 TX	0.10	5.0 sv	14	0.07	5.1 sv	14	0.12	5.0 sv	14
4) TAFT DH300 TX	-0.42	3.2 sv	14	-0.17	3.9 sv	14	0.49	3.0 sv	14
TAFT DH1000 TX	0.17	5.4 sv	14	0.03	5.8 sv	14	0.45	4.4 sv	14

All parameters are from 158 West

⁺ Significant at the 0.1 % level

^{*} Significant at the 1 % level

TABLE IC
COMPARISONS WITH SEA LEVEL NEAR THE SEC RIDGE

	(18S, 150W) PAPEETE SEA LEVEL			(9S, 158W) PENRHYN SEA LEVEL		
	R	STD. ERROR	NO. PTS.	R	STD. ERROR	NO. PTS.
1.) AXBT SH300 RIDGE (steric cm)	0.25	3.1	8	0.93+	1.2	8
AXBT SH300 RIDGE all longitudes	-0.08	4.1	32	0.81+	1.9	30
XBT SH300 RIDGE (steric cm)	0.27	4.6	14	0.31	4.5	14
CTD DH300 RIDGE (dynamic cm)	0.15	3.2	14	0.43	2.6	14
CTD DH1000 RIDGE (dynamic cm)	0.41	3.5	14	0.25	4	14
2.) CTD D14 TROUGH (meters)	-0.03	12	14	0.37	10	14
3.) AXBT SH300 TX (sverdrups)	0.77	3.1	6	0.23	6.1	6
AXBT SH300 TX all longitudes	0.44	5.4	25	0.22	7	23
XBT SH300 TX (sverdrups)	0.56	7.6	11	0.45	8.3	10
CTD DH300 TX (sverdrups)	0.77*	4.9	13	0.24	7.8	11
CTD DH1000 TX (sverdrups)	0.64	12.9	13	0.61	13.8	11

TABLE IC. (CONTINUED) COMPARISONS WITH
SEA LEVEL NEAR THE SEC RIDGE

	(18S, 150W) PAPEETE SEA LEVEL			(9S, 158W) PENRHYN SEA LEVEL		
	R	STD. ERROR	NO. PTS.	R	STD. ERROR	NO. PTS.
4.) TAFT DH300 TX (sverdrups)	0.70*	7.6	14	0.30	11.4	14
TAFT DH1000 TX (sverdrups)	0.53	9	14	0.23	11.5	14

(all parameters were determined from measurements
taken only along 150 West except AXBT parameters)

+ significant at the 0.1% level

* significant at the 1% level

TABLE ID
COMPARISONS WITH SEA LEVEL NEAR THE SEC TROUGH

	(0S, 160W) JARVIS SEA LEVEL			(4S, 155W) MALDEN SEA LEVEL		
	R	STD. ERROR	NO. PTS.	R	STD. ERROR	NO. PTS.
1.) AXBT SH300 TROUGH (steric cm)	0.64+	3.7	32	0.55*	4.4	30
XBT SH300 TROUGH (steric cm)	0.85+	3	14	0.70*	4.3	12
CTD DH300 TROUGH (dynamic cm)	0.81+	3.4	14	0.63	4.9	12
CTD DH1000 TROUGH (dynamic cm)	0.82+	3.6	14	0.59	5.8	12
2.) CTD D14 RIDGE (meters)	0.82+	10	14	0.64	16	12
3.) AXBT SH300 TX (sverdrups)	-0.40	5.6	25	-0.40	6.3	24
XBT SH300 TX (sverdrups)	-0.25	9.8	11	-0.12	10.3	9
CTD DH300 TX (sverdrups)	-0.77*	4.9	13	-0.53	7.7	11
CTD DH1000 TX (sverdrups)	-0.66	12.5	13	-0.48	13.7	11

TABLE ID. (CONTINUED) COMPARISONS WITH
SEA LEVEL NEAR THE SEC TROUGH

	(0S, 160W) JARVIS SEA LEVEL			(4S, 155W) MALDEN SEA LEVEL		
	R	STD. ERROR	NO. PTS.	R	STD. ERROR	NO. PTS.
4.) TAFT DH300 TX (sverdrups)	-0.68*	7.8	14	-0.37	11.9	12
TAFT DH1000 TX (sverdrups)	-0.60	8	14	-0.19	13	12
5.) PCM TX (sverdrups)	-0.19	13	37	0.14	14	31

(all parameters were determined from measurements taken only along 150 West except AXBT and PCM parameters which were from 150 West, 153 West, and 158 West)

+ significant at the 0.1% level

* significant at the 1% level

TABLE IE
CORRELATIONS FOR COMPARISONS AMONG SEA LEVEL
AT SEVERAL ISLAND STATIONS

CHRISTMAS -----	JARVIS -----	MALDEN -----	PENRHYN -----	PAPEETE -----	
0.86+	0.77+	0.68+	0.32*	-0.63+	FANNING
	0.87+	0.84+	0.24	-0.56+	CHRISTMAS
		0.81+	0.26	-0.48+	JARVIS
			0.48*	-0.64+	MALDEN
				-0.10	PENRHYN
	HONOLULU -----	JOHNSTON -----			
	0.69+ (0.87+)	0.56+ (0.83*)		HILO	
		0.70+ (0.91+)		HONOLULU	

(Parenthesis indicate correlations during AXBT flights
along 158 West)

+ significant at the 0.1% level

* significant at the 1% level

B. COMPARISONS BETWEEN SEA LEVEL DIFFERENCES AND
TRANSPORT ESTIMATES FOR THE SEC AND UC

Sea level at Jarvis was subtracted from sea level at Papeete, Penrhyn, and Malden and the difference was then compared with geostrophic transports relative to 300 and 1000 meters for the SEC along 150 West (Table II).

Comparing sea level differences between Papeete and Jarvis with geostrophic transports relative to 300 meters (TAFT DH300 TX) along 150 West gave a high correlation of $R=0.81+$ and a standard error of ± 5.5 SV (see fig. 10).

Comparing sea level differences between Malden and Jarvis with geostrophic transports relative to 1000 meters (TAFT DH1000 TX) along 150 West resulted in a correlation of $R=0.76^*$ and a standard error of ± 7 SV, whereas comparing sea level differences between Papeete and Jarvis with TAFT DH1000 TX gave a correlation of $R=0.67^*$ and a standard error of ± 7.5 SV. These two correlations are not significantly different.

Sea level differences did not correlate well with direct measurements of SEC transport. All 3 pairs of sea level stations gave correlations of $R=0.51$ or less and standard errors of about ± 11 SV. This is because PCM measurements for the SEC were only made between 3 North and 3 South.

One surprising find was that sea level difference across the SEC between Penrhyn and Jarvis correlated well with PCM Undercurrent transport across 158 West with a correlation of $R=-0.70^*$ and a standard error of ± 9 SV (see fig. 11). This negative correlation also exists for comparisons between direct measurements of the SEC (between 3 North and 3 South) and Undercurrent (Firing, 1981). One possible explanation is that these opposing currents directly influence each other by exchanging momentum. For example, when the eastward flowing Undercurrent is strong, it inhibits the westward flowing SEC which then becomes weaker, or vice versa.

TABLE II

COMPARING SEA LEVEL DIFFERENCES WITH TRANSPORT ESTIMATES FOR THE SEC AND UC

		150°W TAFT DH300 TX (sv)	150°W TAFT DH1000 TX (sv)	(3°N-3°S) PCM FOR SEC (sv)	158° W UNDER CURRENT (sv)
△ SEA LEVEL PAPEETE MINUS JARVIS (cm)	CORRELATION	0.81 ⁺	0.67 [*]	0.09	0.12
	STD. ERROR	5.5 sv	7.5 sv	14.5 sv	22 sv
	NO. OF PTS	14	14	37	13
△ SEA LEVEL PENRHYN MINUS JARVIS (cm)	CORRELATION	0.73 [*]	0.61	0.51 [*]	-0.70 [*]
	STD. ERROR	6.5 sv	8 sv	10.5 sv	9 sv
	NO. OF PTS	14	14	36	12
△ SEA LEVEL MALDEN MINUS JARVIS (cm)	CORRELATION	0.62	0.76 [*]	0.46 [*]	-0.44
	STD. ERROR	8 sv	7 sv	11 sv	15 sv
	NO. OF PTS.	12	12	31	10

⁺ Significant at the 0.1% level^{*} Significant at the 1% level

C. COMPARISONS BETWEEN DYNAMIC HEIGHTS AND
ISOTHERM DEPTHS AT THE RIDGES AND TROUGHS

Comparisons were made between dynamic heights and isotherm depths at the ridges and troughs of the equatorial currents. The correlations, slopes, and standard errors of the orthogonal regression lines are shown in Table III.

The slope of the regression line for DH300 vs DH1000 is a measure of the percentage of dynamic height fluctuations occurring in the upper 300 meters relative to 1000 meters. For example, the slope of the regression line for DH300 vs DH1000 is 0.96 at the NECC trough and 0.87 at the NECC ridge. This tells us that about 96% of the thermal and salinity variability associated with changes in dynamic height occurs in the upper 300 meters of the NECC trough compared to about 87% at the NECC ridge. In other words, the thermal structure below 300 meters is fairly stable at the trough while thermal variations extend deeper at the ridge. Salinity variations probably play a small role.

One can check the consistency of this method by examining the slopes of the regression lines for CTD D20 vs DH300 and CTD D20 vs DH1000 to see if they agree with the slope of the regression line for DH300 vs DH1000 from the following formula:

$$\text{Slope } \frac{\text{DH300}}{\text{DH1000}} = \text{Slope } \frac{\text{D20}}{\text{DH1000}} / \text{Slope } \frac{\text{D20}}{\text{DH300}}$$

From simple division, one can see that the slope calculated from this formula agrees extremely well with the actual slope for DH300 vs DH1000 at the NECC ridge and trough. This is because D20 correlated very well with DH300 and DH1000 due to the strong baroclinicity of the NECC. DH300 can be estimated from D20 with an accuracy of ± 1.6 dyn cm at the NECC trough and ± 2.2 dyn cm at the NECC ridge while DH1000 can be estimated from D20 with an accuracy of ± 1.9 dyn cm at the NECC trough and ± 3.2 dyn cm at the NECC ridge (see fig. 12). DEL DH1000 can therefore be accurately determined by measuring D20 located in the upper 100 meters of the NECC trough and the upper 200 meters of the NECC ridge.

The same relationship holds true for the NEC and SEC, but the correlations are lower at the ridges so less confidence is placed on those values. For the NEC, the slope of DH300 vs DH1000 tells us that about 86% of the dynamic height fluctuations occur in the upper 300 meters at the NEC trough compared to about 72% at the NEC ridge relative to 1000 meters. CTD measurements relative to 300 meters would therefore capture about 86% of the variability at the NEC trough and 72% of the variability at the NEC ridge assuming that there is no flow below 1000 meters.

The high correlations between dynamic heights and isotherm depths at the NEC trough allow one to estimate

DH300 and DH1000 from CTD D14. DH300 at the NEC trough can be estimated with an accuracy of about ± 2.5 dyn cm while DH1000 at the NEC trough can be estimated from CTD D14 with an accuracy of about ± 2.9 dyn cm.

For the SEC, the slope of DH300 vs DH1000 tells us that about 91% of the dynamic height fluctuations occur in the upper 300 meters at the SEC trough compared to about 76% at the SEC ridge relative to 1000 meters (see fig. 13). DH300 at the SEC trough can be estimated from CTD D14 with an accuracy of about ± 2.9 dyn cm while DH1000 at the SEC trough can be estimated from CTD D14 with an accuracy of about ± 3.3 dyn cm. Correlations are much lower at the ridge, partly due to the small variability of dynamic height there.

Correlations are also shown for DH1000 ridge vs. DH1000 trough. The negative correlations for the NECC and SEC indicates that sea level at the ridge and trough behave in an opposite manner as if there was a pivot in the middle of the current, however, this is not seen for the NEC.

TABLE IIIA
 COMPARISONS BETWEEN DYNAMIC HEIGHTS AND ISOTHERM DEPTHS
 AT THE RIDGE AND TROUGH OF THE NECC

	DH1000 RIDGE	D20 RIDGE	DH1000 TROUGH	D20 TROUGH
DH300 RIDGE	R = 0.96 SLOPE = 0.87	R = 0.93 SLOPE = 3.04 STD ERR 2.2 dyn/cm	/	/
DH1000 RIDGE	/	R = 0.90 SLOPE = 2.64 STD ERR 3.2 dyn/cm	R = -0.45 SLOPE = -0.70	/
DH300 TROUGH	/	/	R = 0.97 SLOPE = 0.96	R = 0.94 SLOPE = 2.68 STD ERR 1.6 dyn/cm
DH1000 TROUGH	/	/	/	R = 0.92 SLOPE = 2.57 STD ERR 1.9 dyn/cm

All comparisons have 42 data points

All correlations are significant at the 0.1% level

TABLE IIIB
 COMPARISONS BETWEEN DYNAMIC HEIGHTS AND ISOTHERM DEPTHS
 AT THE RIDGE AND TROUGH OF THE NEC

	DH1000 RIDGE	D14 RIDGE	DH1000 TROUGH	D 14 TROUGH
DH300 RIDGE	R = 0.86 ⁺ SLOPE = 0.72	R = 0.29 SLOPE = 4.43 STD ERR 3.8 dyn/cm		
DH1000 RIDGE		R = 0.58 SLOPE = 3.18 STD ERR 4.1 dyn/cm	R = 0.28 SLOPE = 1.33	
DH300 TROUGH			R = 0.99 ⁺ SLOPE = 0.86	R = 0.88 ⁺ SLOPE = 2.83 STD ERR 2.5 dyn/cm
DH1000 TROUGH				R = 0.88 ⁺ SLOPE = 2.44 STD ERR 2.9 dyn/cm

All Comparisons have 14 data points

⁺Significant at the 0.1% level

TABLE IIIC

COMPARISONS BETWEEN DYNAMIC HEIGHTS AND ISOTHERM DEPTHS
AT THE RIDGE AND TROUGH OF THE SEC

	DH1000 RIDGE	D14 RIDGE	DH1000 TROUGH	D14 TROUGH
DH300 RIDGE	R = 0.56 SLOPE = 0.76	R = -0.12 STD ERR 3.3 dyn/cm	/	/
DH1000 RIDGE	/	R = 0.09 STD ERR 4.4 dyn/cm	R = -0.60 SLOPE = -1.85	/
DH300 TROUGH	/	/	R = 0.98 ⁺ SLOPE = 0.91	R = 0.86 ⁺ SLOPE = 3.10 STD ERR 2.9 dyn/cm
DH1000 TROUGH	/	/	/	R = 0.85 ⁺ SLOPE = 2.81 STD ERR 3.3 dyn/cm

All comparisons have 14 data points

⁺Significant at the 0.1% level

D. COMPARISONS BETWEEN GEOSTROPHIC TRANSPORTS
AND INDIRECT ESTIMATES OF TRANSPORT

1. North Equatorial Counter Current

a. Comparisons with Geostrophic Transports
relative to 300 meters for the NECC (TAFT DH300 TX)

Geostrophic transports relative to 300 meters (TAFT DH300 TX) were compared with several indirect estimates of transport for the NECC (Table IVA). Comparing TAFT DH300 TX with the two isotherm methods gave good results. The 2-Layer Approximation method (DEL D20 x D20BAR) gave a high correlation of $R=0.92+$ and a standard error of ± 2.6 SV (see fig. 14). This high correlation can be attributed to the strong baroclinicity of the NECC. The 20 degree isotherm is embedded within the intense NECC thermocline located above 300 meters where most of the flow is. Consequently, geostrophic transport relative to 300 meters for the NECC can be estimated very well from measuring D20 at the ridge and trough.

The dynamic height methods also correlated well with TAFT DH300 TX while comparing TAFT DH300 TX with DEL SH300 gave a lower correlation of $R=0.79+$ and a standard error of ± 4.5 SV.

b. Comparisons with Geostrophic Transports relative to 1000 meters for the NECC (TAFT DH1000 TX)

Geostrophic transports relative to 1000 meters (TAFT DH1000 TX) were compared with several indirect methods of estimating transport. Comparing TAFT DH1000 TX with CTD DH1000 TX gave the highest correlation of $R=0.91+$ and a standard error of ± 3.8 SV. Comparing TAFT DH1000 TX with CTD DH300 TX, DEL DH1000, and the two isotherm methods also gave high correlations. Consequently, one can estimate geostrophic transports relative to 1000 meters for the NECC by calculating dynamic heights or measuring D20 at the ridges and troughs.

DEL DH300 and DEL SH300 also correlated well with TAFT DH1000 TX with $R=0.82+$ and $0.77+$ respectively. These correlations are about the same as the correlations found when comparing TAFT DH1000 TX with sea level (Table IA).

c. Comparisons with PCM Measurements for the NECC

Comparing direct currents measured by the PCM with isotherm depth differences (DEL D20) resulted in a correlation of $R=0.76+$ and a standard error of ± 5.9 SV. Comparing PCM measurements with sea level (Table IA), DEL DH300, DEL SH300, and DEL DH1000 gave about the same correlations.

2. North Equatorial Current

a. Comparisons with Geostrophic Transports relative to 300 meters for the NEC (TAFT DH300 TX)

Geostrophic transports relative to 300 meters (TAFT DH300 TX) were compared with several indirect estimates of transport for the NEC (Table IVB). Comparing TAFT DH300 TX with DEL D14 resulted in a fair correlation of $R=0.69^*$ and a standard error of ± 2.4 SV. Comparing TAFT DH300 TX with DEL DH300, DEL DH1000, and DEL SH300 also gave fair correlations of $R=0.60$. In general, these correlations are lower than for the the NECC. This is probably due to the existence of eddies which disrupted the thermal structure during the ship cruises across the NEC.

It thus appears that the simplest method of estimating geostrophic transports in the upper 300 meters is to measure D14 at the ridge and trough of the NEC. This is because the NEC thermocline responds closely to variations in the flow due to the baroclinicity of the NEC, however, this relationship is disrupted due to the presence of eddies near the NEC ridge which decreases the accuracy of monitoring geostrophic transports relative to 300 meters.

b. Comparisons with Geostrophic Transports
relative to 1000 meters for the NEC (TAFT DH1000 TX)

Comparing geostrophic transports relative to 1000 meters (TAFT DH1000 TX) with CTD DH300 TX gave a correlation of $R=0.69^*$ and a standard error of ± 3.3 SV. The two isotherm methods (DEL D14 and DEL D14 x D14BAR) also correlated fairly well with TAFT DH1000 TX with $R=0.65$ and a standard error of ± 3.5 SV.

Comparing TAFT DH1000 TX with DEL SH300 and DEL DH300 resulted in low correlations. This may be due to fluctuations of the NEC below 300 meters.

It appears that the simplest way to accurately monitor geostrophic transports relative to 1000 meters for the NEC is to measure D14 at the ridge and trough, however, the presence of eddies near the NEC ridge decreases the accuracy of this monitoring method.

3. South Equatorial Current

a. Comparisons with Geostrophic Transports
relative to 300 meters for the SEC (TAFT DH300 TX)

In contrast to the NECC and NEC, geostrophic transports relative to 300 meters (TAFT DH300 TX) for the SEC correlated better with steric height differences (DEL SH300) than with the two isotherm methods (Table IVC). This is probably because the T-S relation is tighter for the SEC

(see fig. 9). The isotherm methods cannot always be applied to the SEC since the D14 trough may occasionally be located south of Papeete. Comparing TAFT DH300 TX with DEL SH300 gave a very high correlation of $R=0.96+$ and a standard error of ± 2.5 SV (see fig. 15). Measurements of steric heights near Penrhyn (located near the SEC ridge) and Jarvis (located near the SEC trough) should therefore provide a simple and accurate method of estimating geostrophic transports in the upper 300 meters of the SEC.

b. Comparisons with Geostrophic Transports
relative to 1000 meters for the SEC (TAFT DH1000 TX)

In contrast to the NEC, dynamic and steric height differences appear to be better at estimating geostrophic transports relative to 1000 meters (TAFT DH1000 TX) than the two isotherm depth methods. This is again due to a tighter T-S relation for the SEC. DEL SH300 correlated well with TAFT DH1000 TX with $R=0.76^*$ and a standard error of ± 6.4 SV whereas the two isotherm methods gave lower correlations. Comparing TAFT DH1000 TX with DEL D14 gave a correlation of $R=0.64$ while comparing TAFT DH1000 TX with DEL D14 x D14BAR gave an even lower correlation of $R=0.45$. This discrepancy in correlations for the two isotherm methods suggests that D14BAR is variable in the SEC. In other words, the average depth of D14 (D14BAR) fluctuates in the SEC.

TABLE IVA

COMPARISONS BETWEEN GEOSTROPHIC TRANSPORTS AND INDIRECT ESTIMATES OF TRANSPORT FOR THE NECC

	CTD DH1000 TX	Δ DH300	Δ DH1000	XBT Δ SH300	CTD Δ D20	CTD Δ D20* $\overline{D20}$	TAFT DH300 TX	TAFT DH1000 TX	PCM
CTD DH300 TX	0.86	0.95	0.93	0.86	0.95	0.97	0.93 +/-2.4sv	0.87 +/-4.4sv	0.70 +/-6.3sv
CTD DH1000 TX		0.86	0.94	0.83	0.85	0.83	0.89 +/-3.0sv	0.91 +/-3.8sv	0.66 +/-6.6sv
Δ DH300			0.98	0.93	0.97	0.93	0.86 +/-3.5sv	0.82 +/-5.2sv	0.73 +/-6.3sv
Δ DH1000				0.92	0.94	0.90	0.88 +/-3.2sv	0.87 +/-4.4sv	0.72 +/-6.5sv
XBT Δ SH300					0.95	0.90	0.79 +/-4.5sv	0.77 +/-5.9sv	0.72 +/-6.4sv
CTD Δ D20						0.98	0.89 +/-3.1sv	0.83 +/-5.0sv	0.76 +/-5.9sv
CTD Δ D20* $\overline{D20}$							0.92 +/-2.6sv	0.84 +/-4.9sv	0.74 +/-5.6sv

PCM comparisons have 30 data points, all other comparisons have 40 or more data points

All correlations are significant at the 0.1 % level

TABLE IVB

COMPARISONS BETWEEN GEOSTROPHIC TRANSPORTS AND INDIRECT ESTIMATES OF TRANSPORT FOR THE NEC

	CTD DH1000 TX	Δ DH300	Δ DH1000	XBT Δ SH300	CTD Δ D14	CTD Δ D14* $\overline{D14}$	TAFT DH300 TX	TAFT DH 1000TX
CTD DH300 TX	0.70	0.71	0.82	0.58	0.83	0.75	0.40 +/-3.1sv	0.69* +/-3.3sv
CTD DH1000 TX		0.29	0.62	0.13	0.63	0.75	0.18 +/-3.8sv	0.70* +/-3.2sv
Δ DH300			0.91	0.71	0.53	0.40	0.59 +/-2.7sv	0.43 +/-4.5sv
Δ DH1000				0.68	0.69	0.63	0.60 +/-2.7sv	0.57 +/-3.9sv
XBT Δ SH300					0.81	0.67	0.59 +/-2.7sv	0.35 +/-4.7sv
CTD Δ D14						0.93	0.69* +/-2.4sv	0.64 +/-3.5sv
CTD Δ D14* $\overline{D14}$							0.49 +/-3.0sv	0.65 +/-3.5sv

All comparisons have 13 or more data points

+ Significant at the 0.1 % level

* Significant at the 1 % level

TABLE IVC

COMPARISONS BETWEEN GEOSTROPHIC TRANSPORTS AND INDIRECT ESTIMATES OF TRANSPORT FOR THE SEC

	CTD DH1000 TX	Δ DH300	Δ DH1000	XBT Δ SH300	CTD Δ D14	CTD Δ D14* $\overline{\Delta$ D14	TAFT DH300 TX	TAFT DH1000 TX
CTD DH300 TX	0.77	0.93	0.90	0.87	0.77	0.53	0.83 ⁺ +/-5.0sv	0.63 +/-8.0sv
CTD DH1000 TX		0.78	0.86	0.74	0.61	0.41	0.69 [*] +/-7.0sv	0.57 +/-8.8sv
Δ DH300			0.97	0.93	0.72	0.55	0.91 ⁺ +/-3.5sv	0.75 [*] +/-6.6sv
Δ DH1000				0.90	0.81	0.61	0.91 ⁺ +/-3.5sv	0.74 [*] +/-6.7sv
XBT Δ SH300					0.41	0.29	0.96 ⁺ +/-2.5sv	0.76 [*] +/-6.4sv
CTD Δ D14						0.93	0.84 ⁺ +/-5.0sv	0.64 +/-7.9sv
CTD Δ D14* $\overline{\Delta$ D14							0.66 [*] +/-7.0sv	0.45 +/-9.7sv

All comparisons have 12 or more data points

⁺Significant at the 0.1 % level^{*}Significant at the 1 % level

E. COMPARISONS BETWEEN XBT AND CTD
MEASUREMENTS 1/2 DEGREE APART

1.) XBT isotherm depths vs. CTD isotherm depths
at the ridges and troughs

Isotherm depths were measured every 1/2 degree, alternating between XBT and CTD instruments, in other words, the two data sets were sampled at one degree intervals but are offset by 1/2 degree. CTD's are considered to be very accurate in determining isotherm depths while XBT's measure isotherm depths with an accuracy of about 10 meters (Heinmiller, 1983). By examining the relationship between XBT isotherm depths and CTD isotherm depths at the ridges and troughs, one can estimate the error associated with determining isotherm depth extremes at the ridges and troughs from sampling at one degree intervals with an XBT (Table V). The standard error is used as a measure of accuracy.

a.) NECC Ridge and Trough

D20 fluctuated between 110 and 180 meters at the NECC ridge and 40 and 100 meters at the NECC trough. There was a high correlation at both the ridge and trough ($R=0.93$ and 0.87). From the standard error, XBT isotherm depth extremes were accurate to within ± 7 meters at the NECC ridge and trough.

b.) NEC and SEC Trough

D14 fluctuated between 80 and 130 meters at the NEC trough and 130 and 190 meters at the SEC trough. Correlations were lower ($R=0.84$ and 0.76) but XBT isotherm depth extremes were still accurate to within ± 8 meters at the NEC trough and ± 11 meters at the SEC trough.

c.) NEC and SEC Ridge

D14 fluctuated between 250 and 300 meters at the NEC ridge and 340 and 370 meters at the SEC ridge. The correlation was high at the NEC ridge ($R=0.79$) but low at the SEC ridge ($R=-0.02$) since D14 was deeper and fluctuated less at the SEC ridge. From the standard error, XBT isotherm depth extremes were accurate to within ± 14 meters at the NEC and SEC ridge.

In general, determining isotherm depth extremes (D14 and D20) at the ridges and troughs by sampling at one degree intervals with an XBT results in an error of about ± 10 meters. In a worst case situation, estimates of transport from the two isotherm methods (Isotherm Depth Differences and the 2-Layer Approximation Method) would be affected by about 5 SV.

2.) XBT Steric Heights vs. CTD Dynamic Heights
at the ridges and troughs

Steric and dynamic heights were alternately measured every 1/2 degree with XBT and CTD instruments. Steric heights were calculated from XBT's using a mean T-S relation. By examining the relationship between XBT SH300 and CTD DH300 at the ridges and troughs, one can estimate the error associated with determining DH300 at the ridges and troughs from sampling at one degree intervals with an XBT. The standard error is again used as a measure of accuracy.

- a.) NEC Ridge - Dynamic height relative to 300 meters (DH300) at the NEC ridge fluctuated between 103 and 117 dyn cm. This small variation was part of the reason why steric height (SH300) did not correlate well with DH300 ($R=0.59$). SH300 estimated DH300 at the NEC ridge with a standard error of ± 3 dyn cm. The NEC ridge was relatively sharp during the Shuttle Experiment which increased the error due to sampling at one degree intervals instead of 1/2 degree intervals (see fig. 4).

- b.) NECC Trough - DH300 at the NECC trough fluctuated between 66 and 86 dyn cm. SH300 correlated well with DH300 at the NECC trough as indicated by the high correlation ($R=0.85$) and low standard error of ± 3 dyn cm.
- c.) NECC Ridge - DH300 at the NECC ridge fluctuated between 88 and 112 dyn cm. SH300 correlated with DH300 at the NECC ridge even better than at the NECC trough with $R=0.91+$ and a standard error of ± 2.5 dyn cm. This is due to a relatively stable salinity structure near 4 North (see fig. 9b).
- d.) SEC Trough - DH300 at the SEC trough fluctuated between 79 and 96 dyn cm. SH300 correlated very well with DH300 at the SEC trough with $R=0.95+$ and a standard error of ± 1.6 dyn cm. This high correlation is partly due to the SEC trough being relatively flat which decreases the error due to sampling at one degree intervals instead of $1/2$ degree intervals (see fig. 4).

e.) SEC Ridge - DH300 at the SEC Ridge fluctuated very little between 108 and 115 dyn cm, however, SH300 still correlated fairly well with DH300 at the SEC ridge with $R=0.64$ and a standard error of ± 3 dyn cm. This is due to a relatively stable salinity structure near the SEC ridge (see fig. 9c).

In general, determining DH300 at the ridges and troughs by sampling at one degree intervals with XBT's resulted in an error of about ± 2.5 dyn cm. Part of the reason for the low error is because the mean T-S relation for computing SH300 was constructed from one year of data taken from the Shuttle Experiment itself.

TABLE V
COMPARISONS BETWEEN XBT AND CTD MEASUREMENTS $\frac{1}{2}$ DEGREE APART

	COUNTER CURRENT	NORTH EQ. CURRENT	SOUTH EQ. CURRENT
XBT D14 RIDGE VS. CTD D14 RIDGE	R = 0.93 ⁺ Std error 6.3 meters	R = 0.79 ⁺ Std Error 11 meters	R = -0.02 Std error 14 meters
XBT D14 TROUGH VS. CTD D14 TROUGH	R = 0.87 ⁺ Std error 7 meters	R = 0.84 ⁺ Std error 7.6 meters	R = 0.76 [*] Std error 11 meters
XBT SH300 RIDGE VS. CTD DH300 RIDGE	R = 0.91 ⁺ Std error 2.5 dyn cm	R = 0.59 Std error 2.8 dyn cm	R = 0.64 Std error 2 dyn cm
XBT SH300 TROUGH VS. CTD DH300 TROUGH	R = 0.85 ⁺ Std error 2.5 dyn cm	R = 0.88 ⁺ Std error 2.4 dyn cm	R = 0.95 ⁺ Std error 1.6 dyn cm
NUMBER OF POINTS	42	14	14

⁺ Significant at the 0.1 % level

^{*} Significant at the 1 % level

F. ZONAL VARIABILITY OF THE NECC

The sampling pattern for the Shuttle Experiment included measurements along three meridional sections (150W, 153W, and 158W). The decision to monitor these three adjacent sections was inspired by Test Shuttle observations (Barnett and Patzert, 1980) which showed some surprising differences in ocean structure between 150 West and 158 West.

Comparisons between different transport estimates for the NECC resulted in correlations which were significantly different for the three meridional sections (see Table VI). In general, the correlations obtained along 158 West seem to be lower than those obtained along 150 West and 153 West.

One plausible explanation is that the islands located near 158 West somehow interfere with the dynamics of equatorial circulation. The islands of Palmyra, Fanning, Christmas, and Jarvis are all located within a few degrees of 158 West. It therefore seems possible that this "island effect" is what is responsible for the lower correlations along 158 West.

TABLE VI
ZONAL VARIABILITY OF THE NECC

	<u>150 WEST</u>	<u>153 WEST</u>	<u>158 WEST</u>
CTD DH1000 TX VS. ISOTH METHOD	0.84 (14)	0.92 (13)	0.66 (13)
CTD DH1000 TX VS. PCM TX	0.86 (12)	0.65 (9)	0.48 (10)
DEL DH1000 VS. ISOTH METHOD	0.96 (14)	0.95 (14)	0.77 (14)
TAFT DH1000 TX VS. ISOTH METHOD	0.90 (14)	0.91 (14)	0.73 (14)
DEL DH300 VS. PCM TX	0.79 (12)	0.79 (10)	0.55 (11)
TAFT DH1000 TX VS. PCM TX	0.87 (12)	0.77 (10)	0.53 (11)
FANNING SL VS. PCM TX	0.55 (12)	0.64 (10)	0.31 (11)

(NUMBERS IN PARENTHESIS ARE THE NUMBER OF DATA POINTS)

G. SOURCES OF ERROR

The main source of error in estimating geostrophic transport is due to ageostrophy. Eddies, meanders, and internal waves can alter the dynamics of equatorial current circulation. High frequency internal waves can cause large fluctuations of isotherm surfaces. There is also evidence of a 4-6 day barotropic, planetary oscillation in the Pacific Ocean (Luther, 1982). 3 - 5 day waves have been found to exist in the equatorial current system (Wunsch and Gill, 1976) which can cause large fluctuations of isotherm depths over short periods. Previous studies showed that the 18 degree isotherm depth frequently changed by more than 20 meters in less than one day (Wyrтки et al., 1977). 30-day waves are also known to exist in the NECC (Legeckis, 1977). The higher frequency phenomena would tend to disrupt the relationships found between different methods of estimating transports. For low frequency monitoring, it would be desirable to filter out these effects.

Another source of error comes from using a mean T-S relation to calculate steric height from XBT and AXBT measurements. For the shuttle cruises, 80% of the steric heights were within +/- 1 dyn cm of the actual dynamic height. This error would be greater during an El Nino when salinity anomalies are significant. One method of reducing

this error would be to incorporate surface salinity into the calculations of steric heights (Kessler, unpubl).

Isotherm depths used in estimating transport are also subject to an error of about 10 meters for the XBT (Heinmiller, 1983).

Estimating geostrophic transport from measurements only at the ridge and trough can introduce significant errors if the dynamic height slope is skewed instead of linear. If the dynamic height slope is skewed toward the equator, this could result in a significant increase in geostrophic transport, especially at low latitudes.

Different types of errors are associated with direct measurements. Measuring direct currents from points located far apart in a highly variable field of motion is one problem. The quality of the PCM profile itself is dependent on many factors such as the stability of the ship, wire angle, and rocking motions. Estimating the accuracy of PCM profiles is difficult but they are roughly accurate to about 20 cm/s. There were also missing data points in the PCM sections due to bad profiles. These gaps were handled by interpolation if the gap was not too large. Because of these uncertainties, less confidence was placed on PCM transport values.

VI. CONCLUSIONS

A scientific method for monitoring the transports of the equatorial currents based on simple observations of the thermal structure and sea level was developed from data taken during the Hawaii to Tahiti Shuttle Experiment conducted between January 1979 and June 1980. Geostrophic transports relative to 300 and 1000 meters were compared with measurements of isotherm depths and sea level and calculations of steric heights, dynamic heights, and approximate geostrophic transports to determine the most accurate monitoring method (Table VII). It was found that islands may disrupt the relationships found among the different transport indices but geostrophic transports can still be monitored well near islands and even better away from them.

Geostrophic transports for the NECC and NEC can be simply and accurately monitored by measuring isotherm depths at the ridges and troughs. This is due to the strong baroclinicity of these currents. The NECC transports can be monitored with an accuracy of about ± 2.5 SV for transports relative to 300 meters and ± 5 SV for transports relative to 1000 meters by measuring D20 at the ridges and troughs. The NEC transports can be monitored with an accuracy of about ± 2.5 SV for transports relative

to 300 meters and ± 3.5 SV for transports relative to 1000 meters by measuring D14 at the ridges and troughs.

Geostrophic transports for the SEC can be monitored fairly well by calculating steric heights relative to 300 meters at the ridges and troughs. This is because the T-S relation is relatively tight for the SEC. The SEC transports can be monitored with an accuracy of about ± 2.5 SV for transports relative to 300 meters and ± 6.5 SV for transports relative to 1000 meters by calculating steric heights relative to 300 meters at the ridges and troughs.

Sea level measurements obtained from tide gauges located on several islands near the equatorial Pacific also provide a fairly reliable method of monitoring geostrophic transports relative to 1000 meters for the NEC (± 4.5 SV), NECC (± 5.5 SV), and SEC (± 7 SV). Geostrophic transports relative to 300 meters can be monitored well from sea level with an accuracy of about ± 3.5 SV for the NECC, ± 3 SV for the NEC, and ± 5.5 SV for the SEC.

No method was found for accurately monitoring the Undercurrent, though meridional sea level differences look somewhat promising.

These simple methods provide an alternative for the more expensive CTD sections but are unproven during anomalous conditions such as an El Nino. These methods rely only on measurements at the ridges and troughs which are

confined within a fairly narrow belt for most of the equatorial currents. This promotes discrete sampling near the ridges and troughs as an economical way of monitoring the transports. It was shown that XBT's can be used to accurately determine isotherm depths and dynamic heights at the ridges and troughs of the equatorial currents by sampling at one degree intervals.

It was found that most of the dynamic height fluctuations were confined to the upper 300 meters of the equatorial currents except near the NEC and SEC ridge. Dynamic heights at the ridges and troughs can be accurately estimated from isotherm depths, especially for the NECC ridge, NECC trough, and SEC trough.

TABLE VII

THE ACCURACY OF ESTIMATING GEOSTROPHIC TRANSPORTS
RELATIVE TO 300 METERS

	ISOTHERM METHODS -----	STERIC HEIGHT DIFFERENCES -----	APPROX. GEOSTROPHIC METHOD -----	SEA LEVEL -----
NECC	2.6 SV	4.5 SV	2.4 SV	4.5 SV
NEC	2.4 SV	2.7 SV	3.1 SV	3.0 SV
SEC	5.0 SV	2.5 SV	5.0 SV	5.5 SV

THE ACCURACY OF ESTIMATING GEOSTROPHIC TRANSPORTS
RELATIVE TO 1000 METERS

	ISOTHERM METHODS -----	STERIC HEIGHT DIFFERENCES -----	APPROX. GEOSTROPHIC METHOD -----	SEA LEVEL -----
NECC	4.9 SV	5.9 SV	3.8 SV	5.5 SV
NEC	3.5 SV	4.7 SV	3.2 SV	4.4 SV
SEC	7.9 SV	6.4 SV	8.0 SV	7.0 SV

APPENDIX

Figures 1 - 15

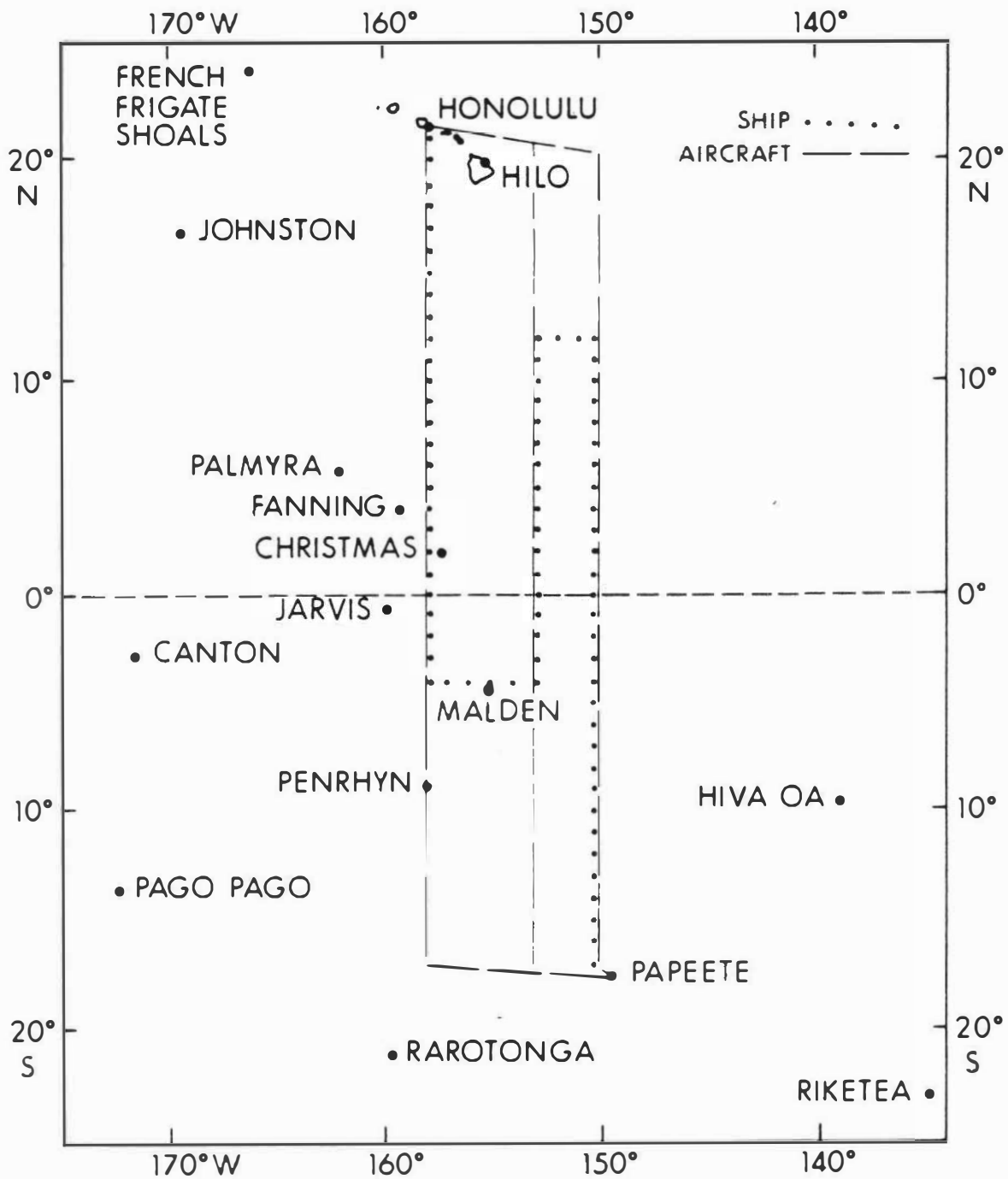


Fig. 1. Location of the Hawaii to Tahiti Shuttle Experiment, showing the ship track, aircraft sections and sea level stations.

(From Wyrтки and Kilonsky, 1982, Fig. 1.)

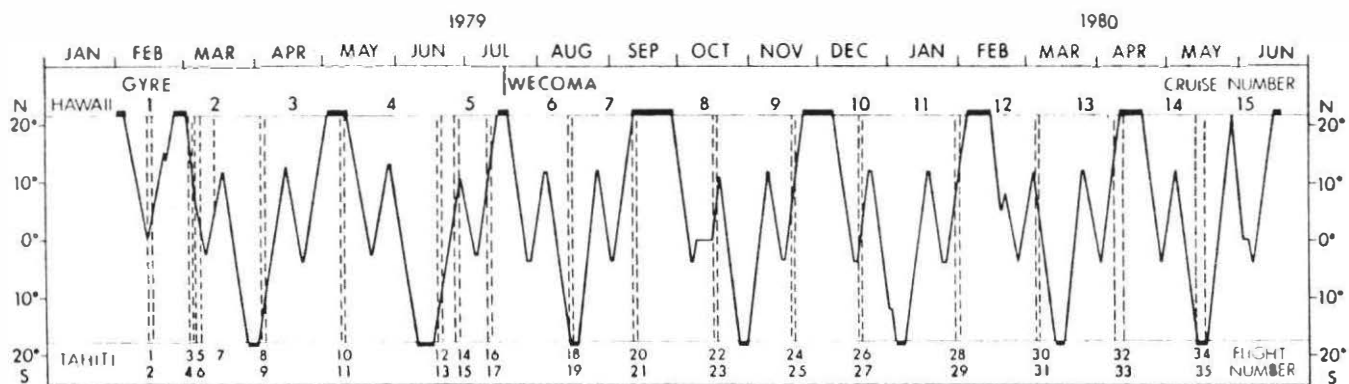


Fig. 2. Time-latitude diagram of the Shuttle Experiment, showing the track of the research vessels Gyre and Wecoma (solid lines) and the flights between Honolulu and Papeete (dashed lines). (From Wyrтки and Kilonsky, 1982, Fig. 2.)

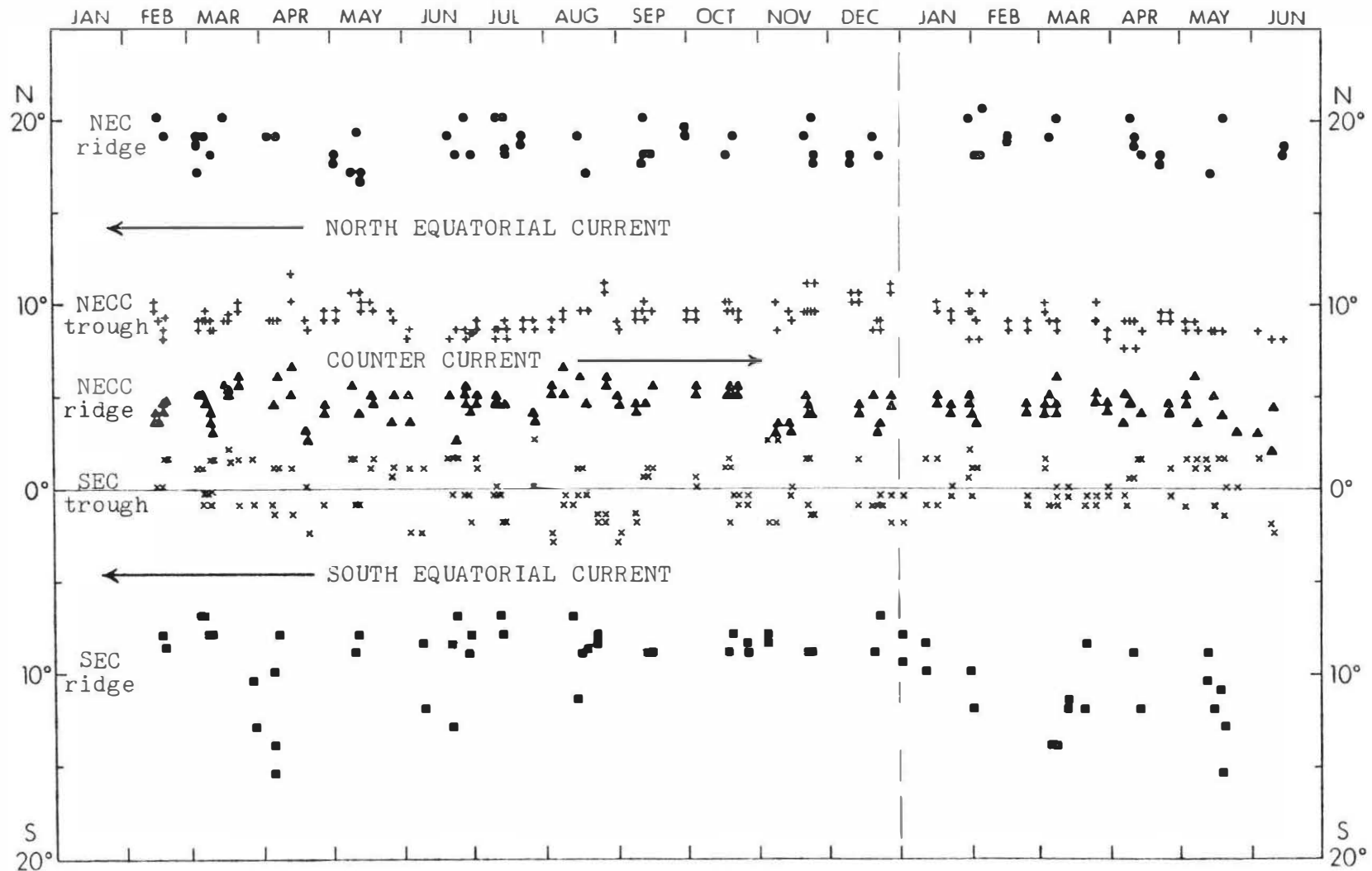


Fig. 3. Positions of the ridges and troughs during the Shuttle Experiment.

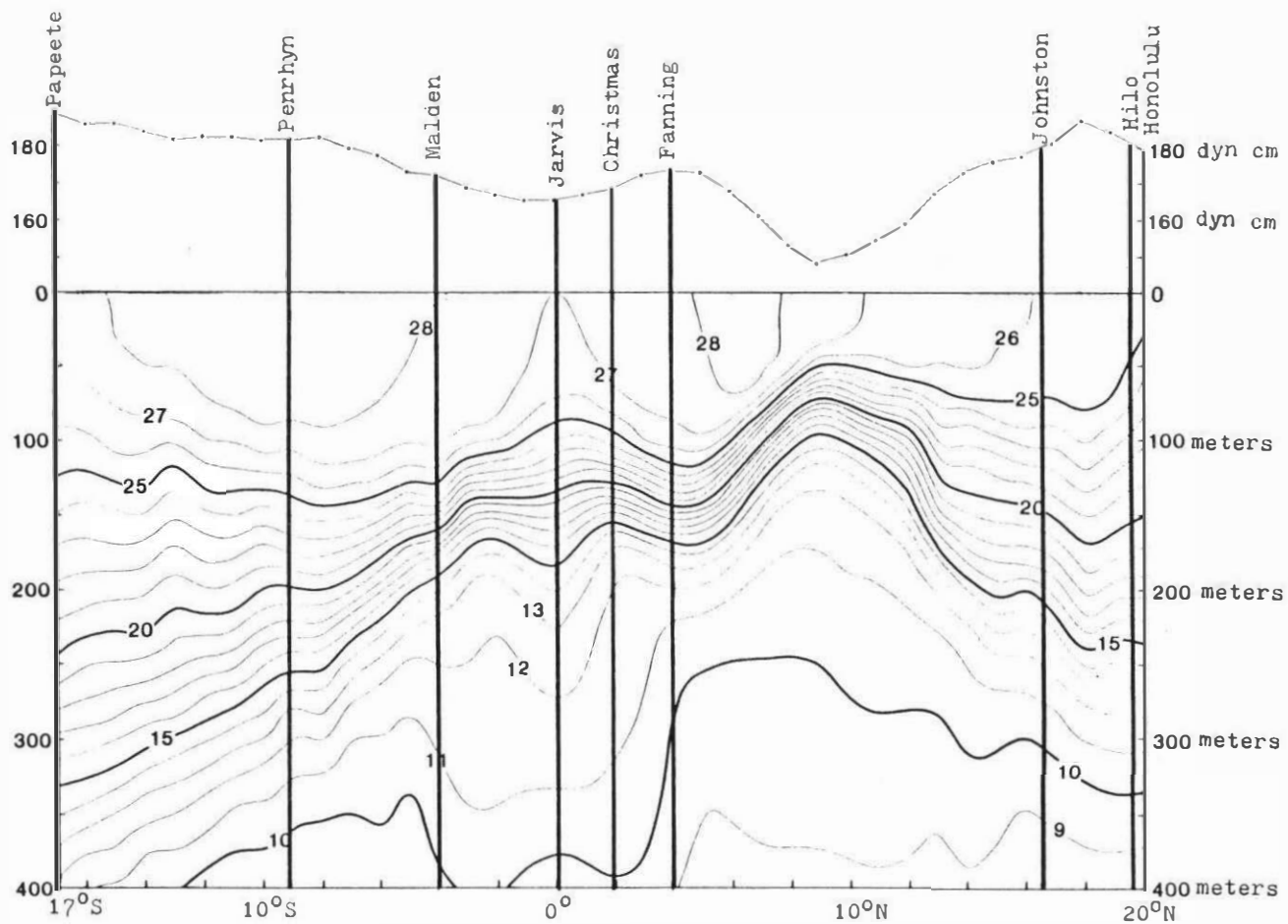
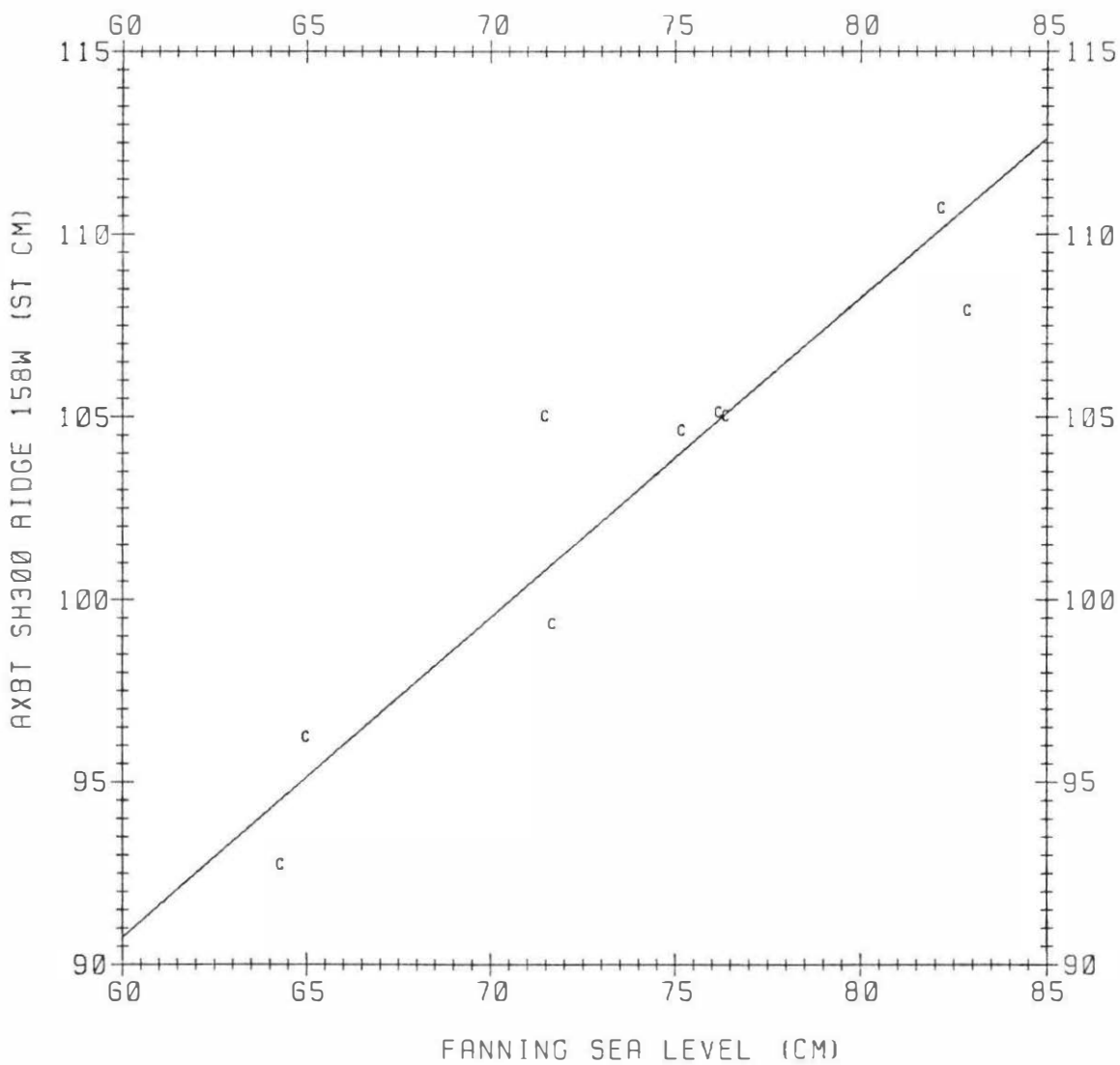


Fig. 4. Temperature ($^{\circ}\text{C}$) from the sea surface to 400 m between Hawaii and Tahiti. Top: Dynamic height topography relative to 1000 meters showing the locations of the sea level island stations. (From Wyrtki and Kilonsky, 1982, Fig. 4.)



COUNTER CURRENT

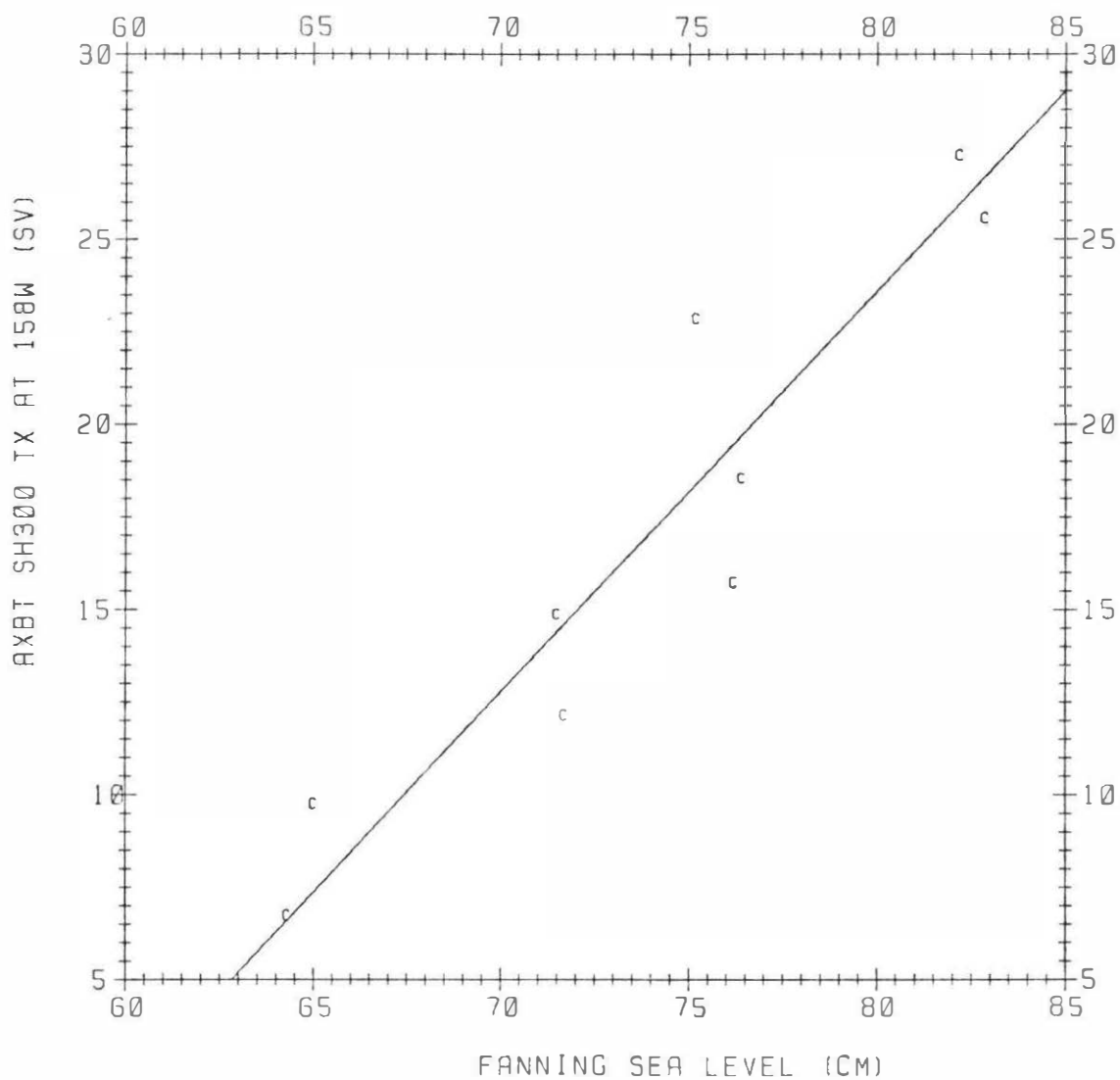
* POINTS = 9

R = 0.94

X-STDERR = 2.5

Y-STDERR = 2.2

Fig. 5. Comparison between Fanning sea level and steric heights calculated from AXBT measurements at the NECC ridge along 158 West.



COUNTER CURRENT

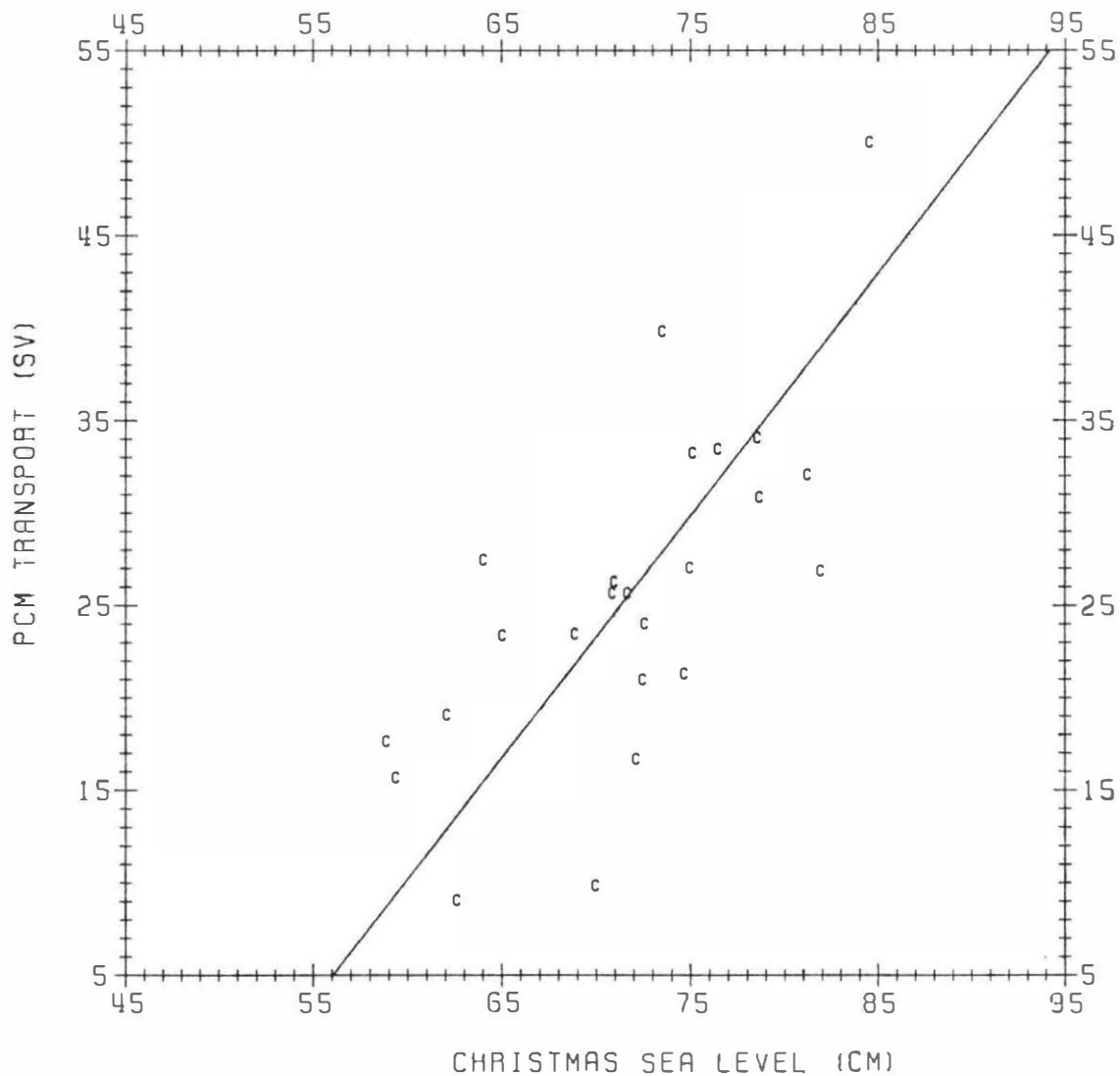
* POINTS = 9

R = 0.94

X-STDERR = 2.5

Y-STDERR = 2.7

Fig. 6. Comparison between Fanning sea level and Approximate Geostrophic transports for the NECC along 158 West calculated from AXBT measurements.



COUNTER CURRENT

* POINTS = 24

R = 0.70

X-STDERR = 5.5

Y-STDERR = 7.3

Fig. 7. Comparison between Christmas Island sea level and direct measurements of the NECC transport.

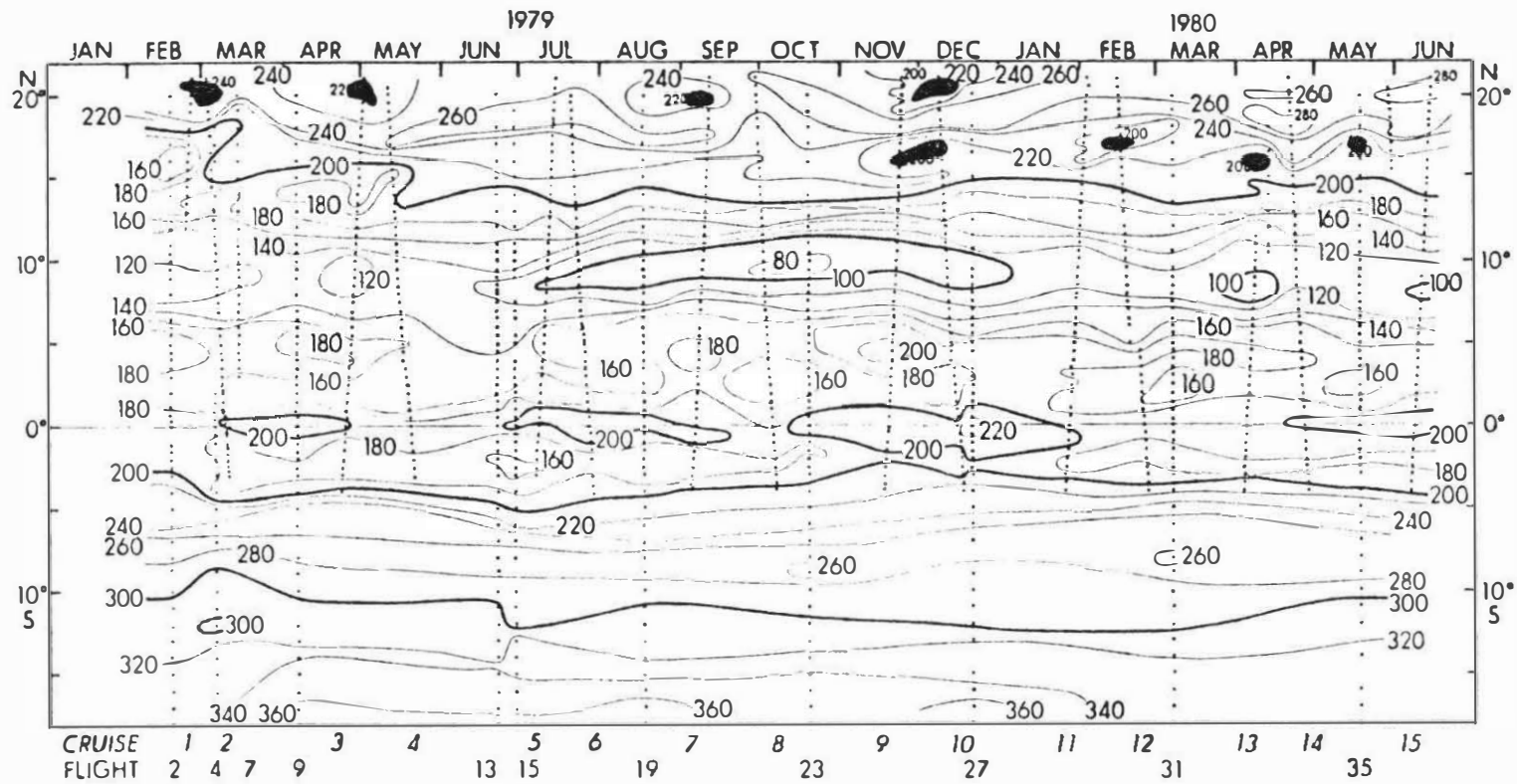
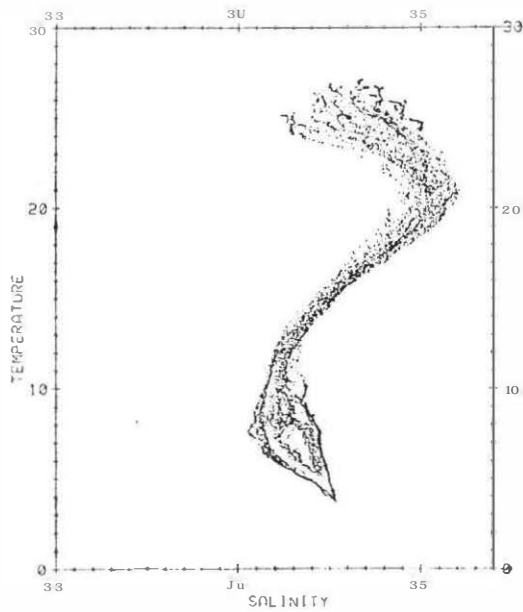
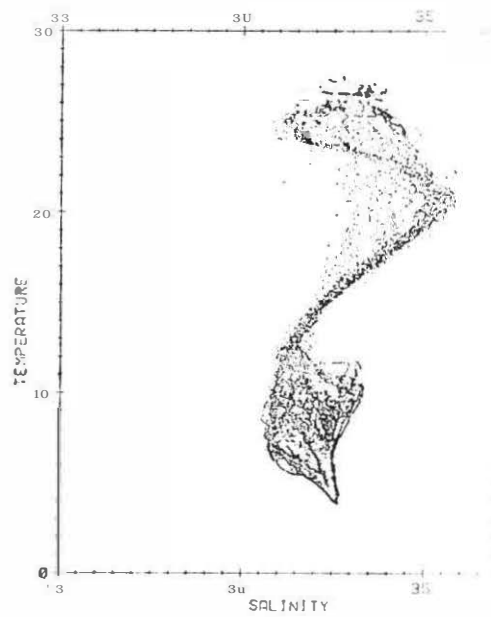


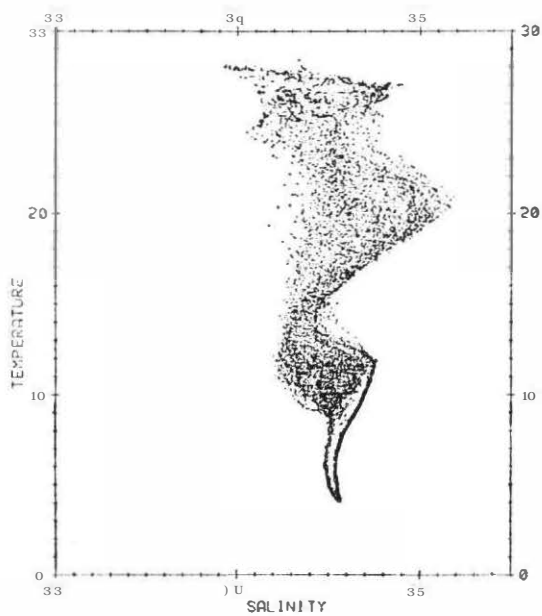
Fig. 8. Depth of the 14°C isotherm in meters along 158°W



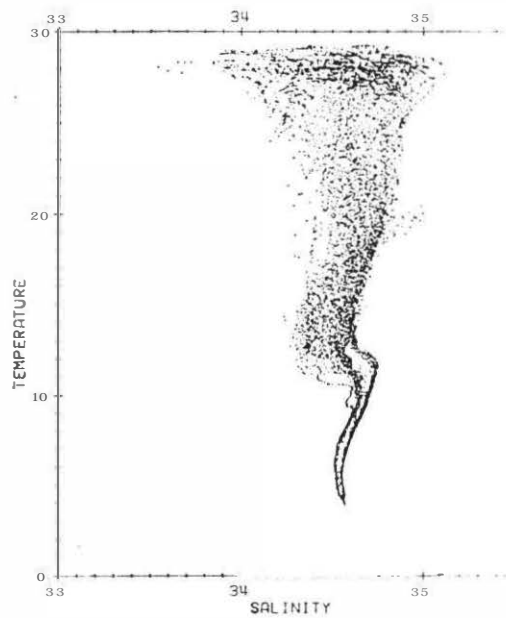
20 North



16 North

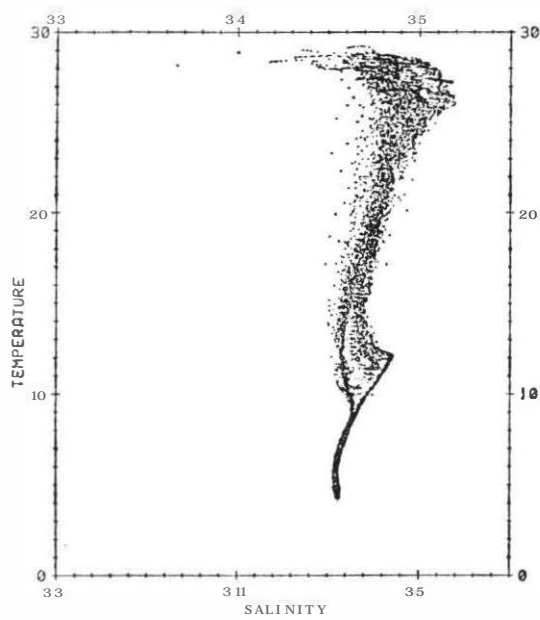


12 North

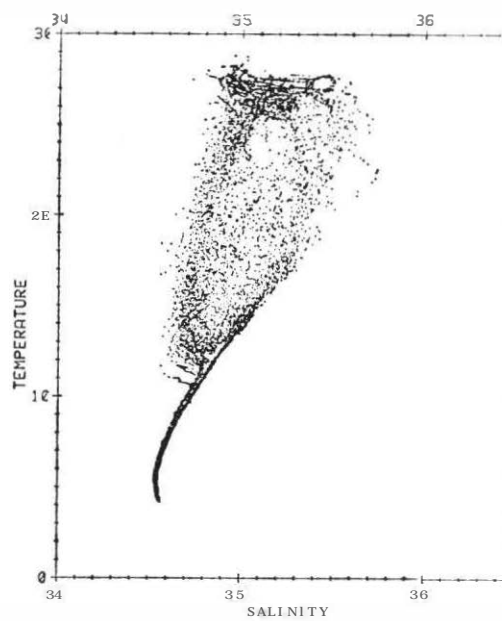


8 North

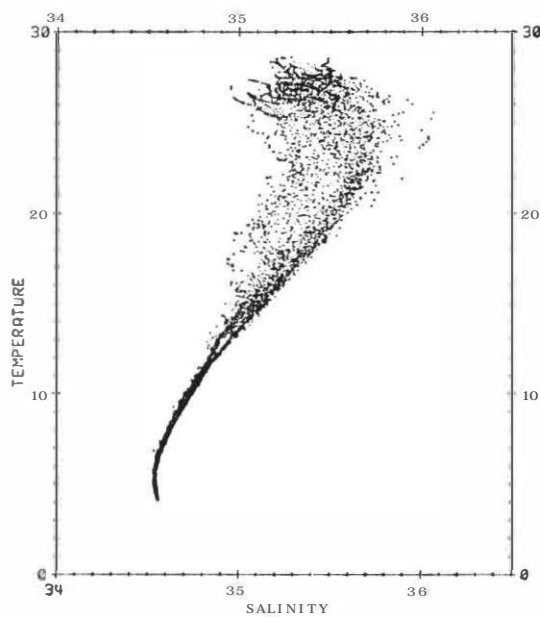
Fig. 9a. Temperature-Salinity relations between 20 North and 8 North during the Shuttle Experiment.



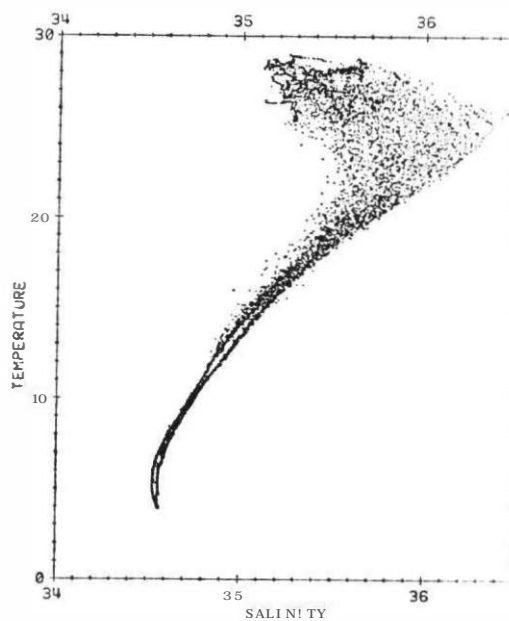
4 North



1 North

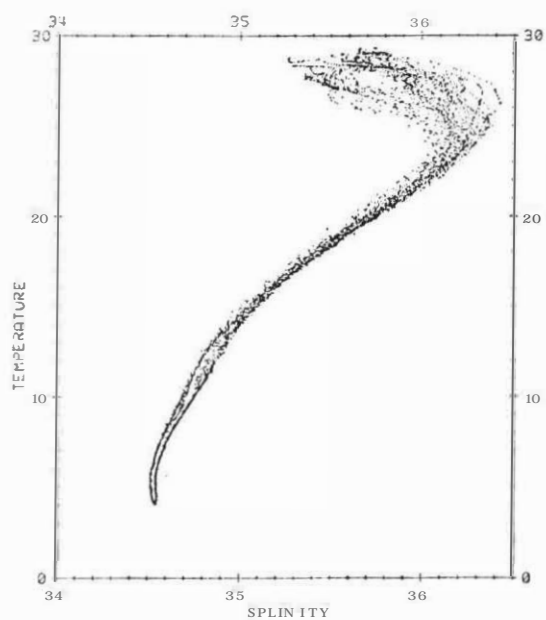


1 South

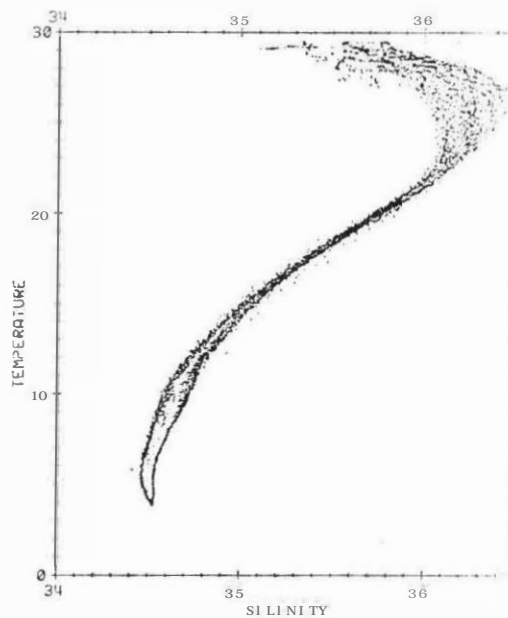


4 South

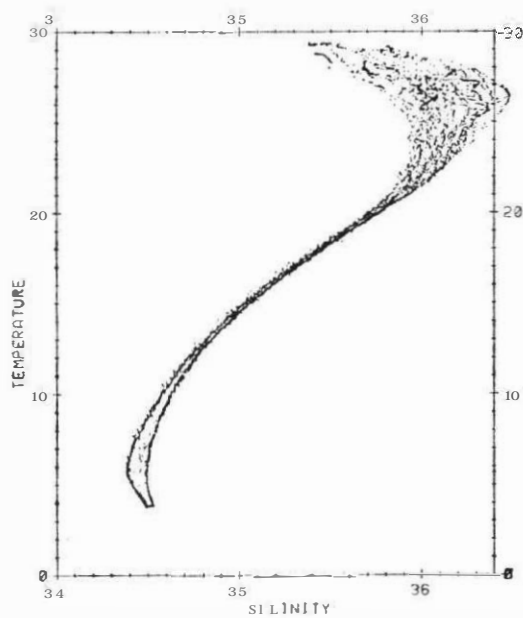
Fig. 9b. Temperature-Salinity relations between 4 North and 4 South during the Shuttle Experiment.



8 South

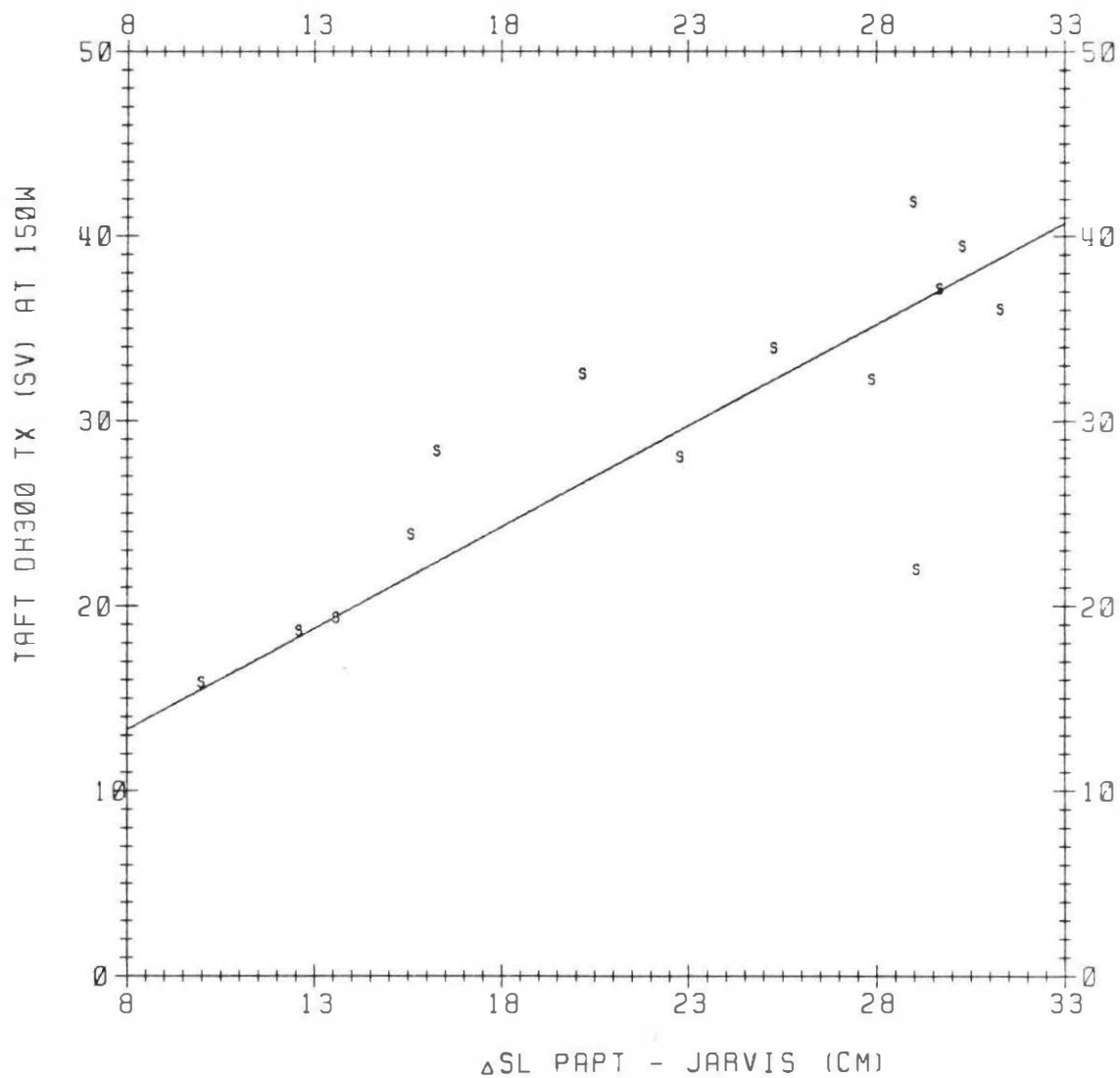


12 South



16 South

Fig. 9c. Temperature-Salinity relations between 8 South and 16 South during the Shuttle Experiment.



SOUTH EQ. CURRENT

* POINTS = 14

R = 0.81

X-STDERR = 4.8

Y-STDERR = 5.3

Fig. 10 Comparing sea level differences between Papeete and Jarvis Island with Taft's calculations of geostrophic transport relative to 300 meters for the SEC along 150 West.

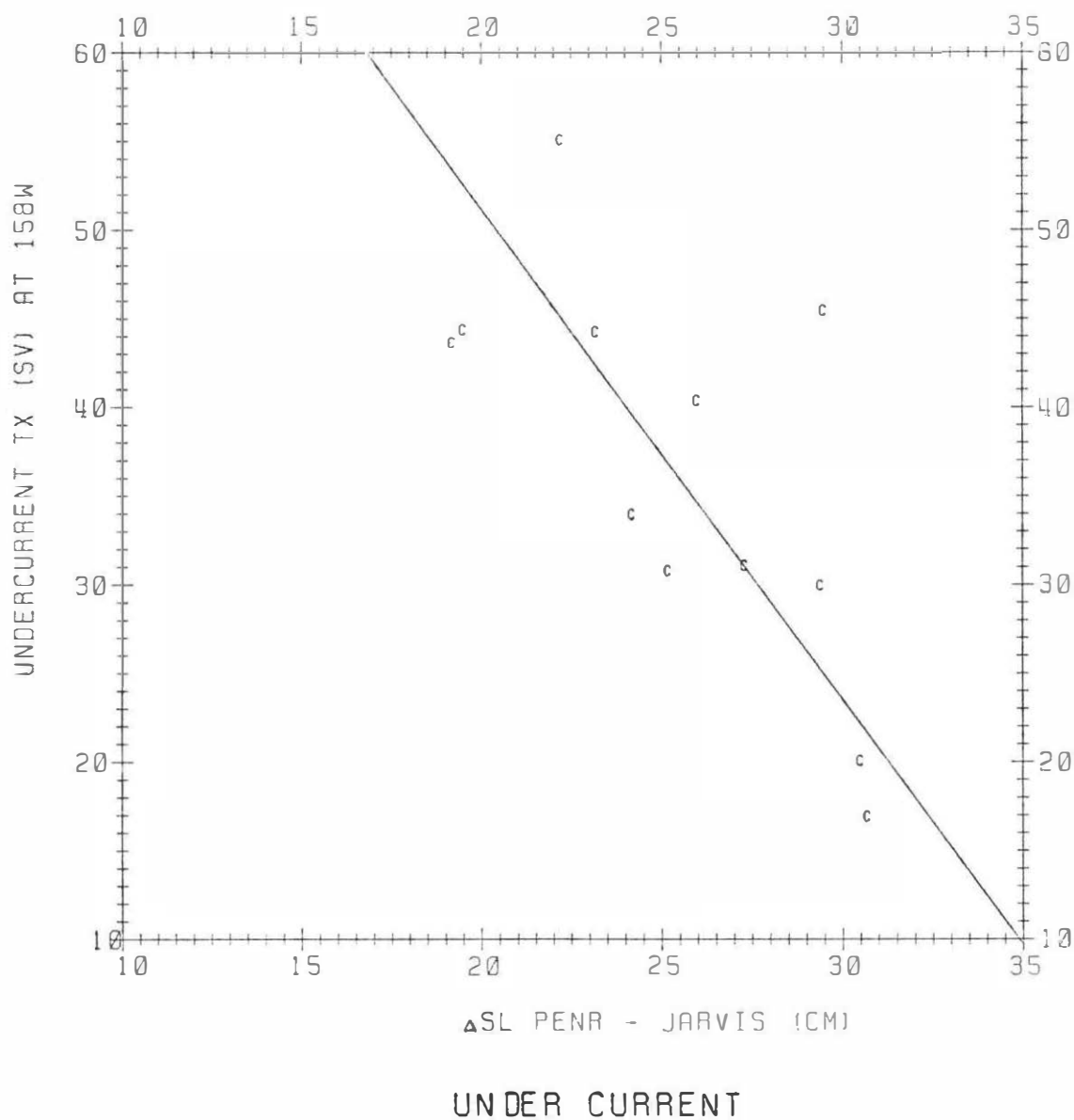
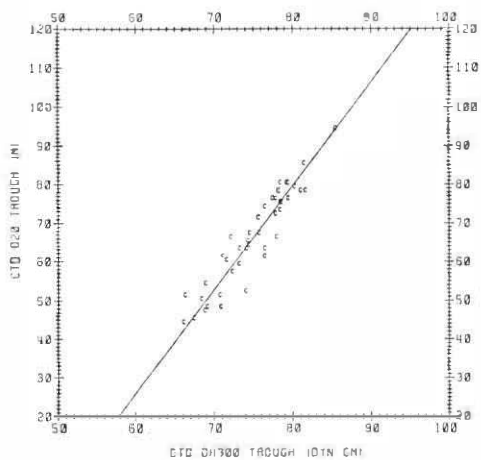
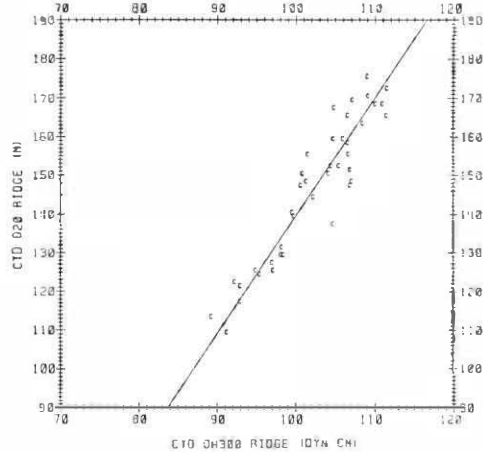


Fig. 11. Comparing sea level differences between Penrhyn and Jarvis island with direct measurements of the Undercurrent transport along 158 West.



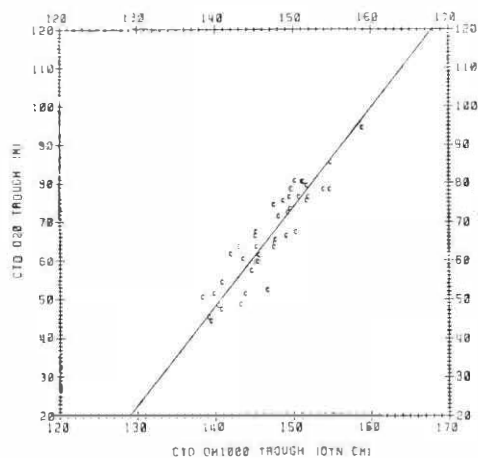
COUNTER CURRENT

SLOPE = 2.7 Y-INTERCEPT = -135.1 R = 0.94
 POINTS = 42 X-STDEVR = 1.0 Y-STDEVR = 11.3



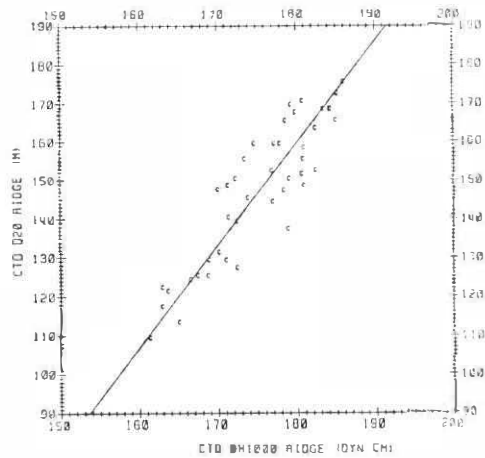
COUNTER CURRENT

SLOPE = 3.8 Y-INTERCEPT = -164.7 R = 0.94
 POINTS = 41 X-STDEVR = 2.2 Y-STDEVR = 5.5



COUNTER CURRENT

SLOPE = 2.6 Y-INTERCEPT = -311.8 R = 0.92
 POINTS = 42 X-STDEVR = 1.8 Y-STDEVR = 9.0



COUNTER CURRENT

SLOPE = 2.6 Y-INTERCEPT = -315.8 R = 0.89
 POINTS = 42 X-STDEVR = 3.2 Y-STDEVR = 8.1

Fig. 12. Comparisons between the 20 degree isotherm depths and dynamic heights relative to 300 and 1000 meters at the ridge and trough of the NECC.

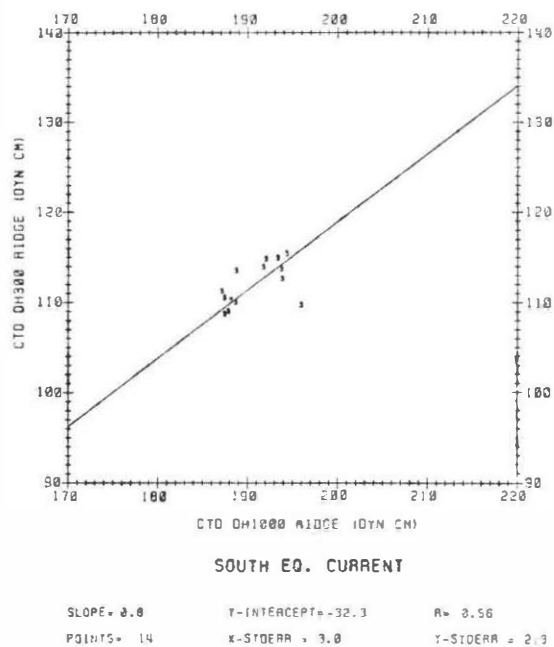
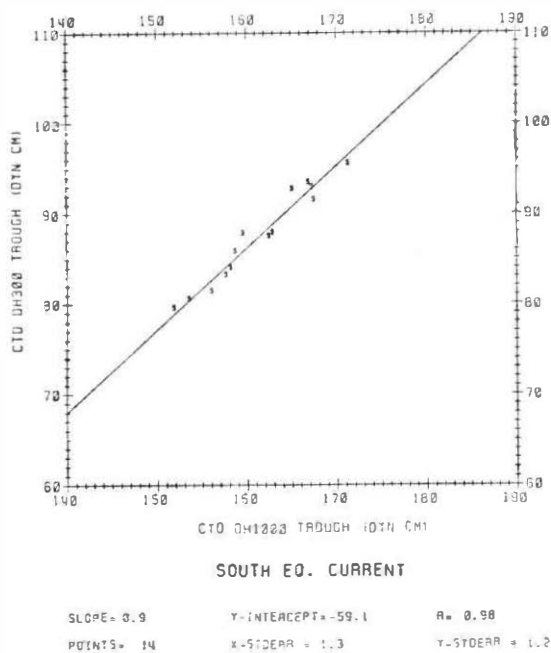
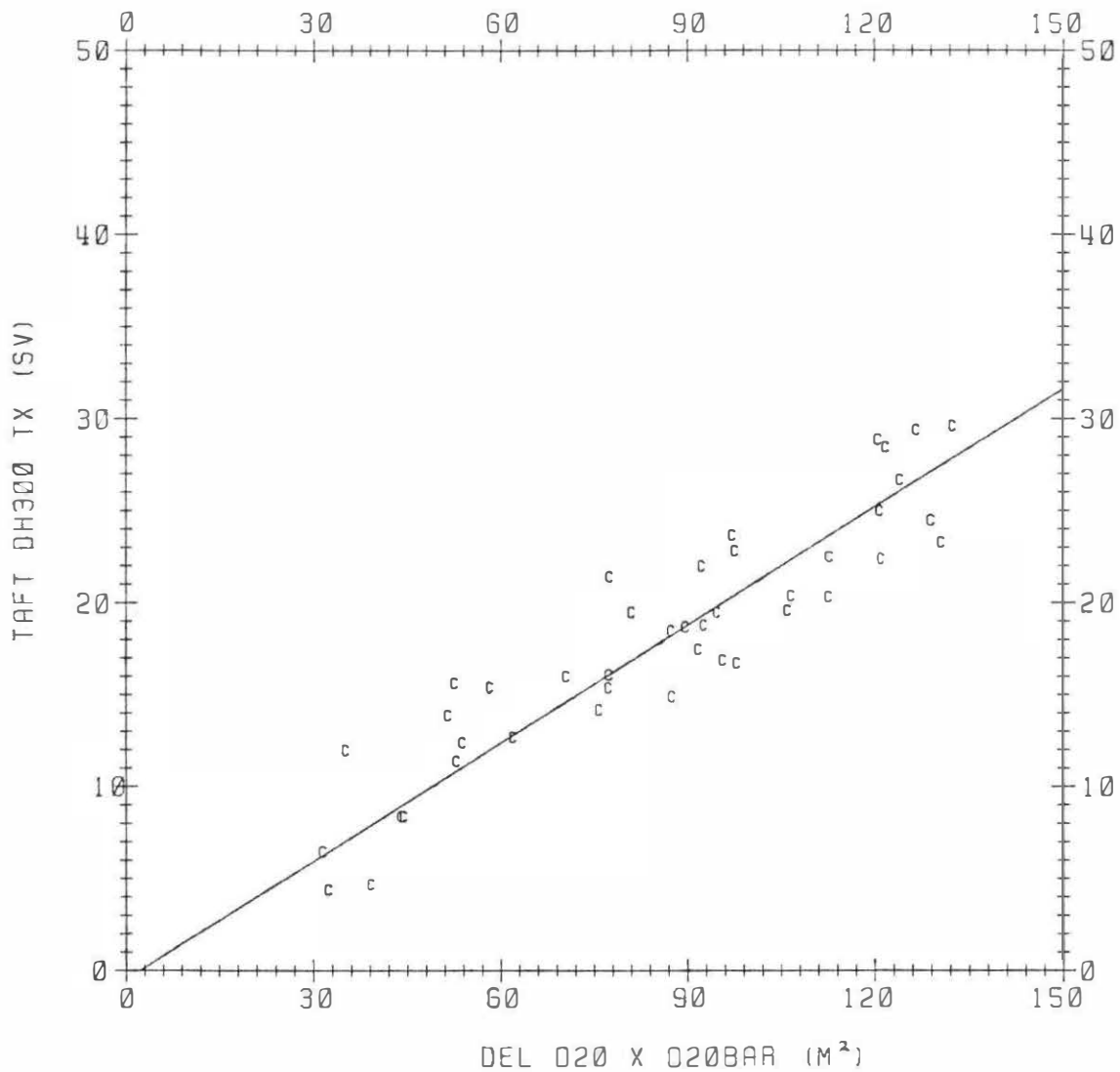


Fig. 13. Comparisons between dynamic heights relative to 300 meters and dynamic heights relative to 1000 meters at the ridge and trough of the SEC.



COUNTER CURRENT

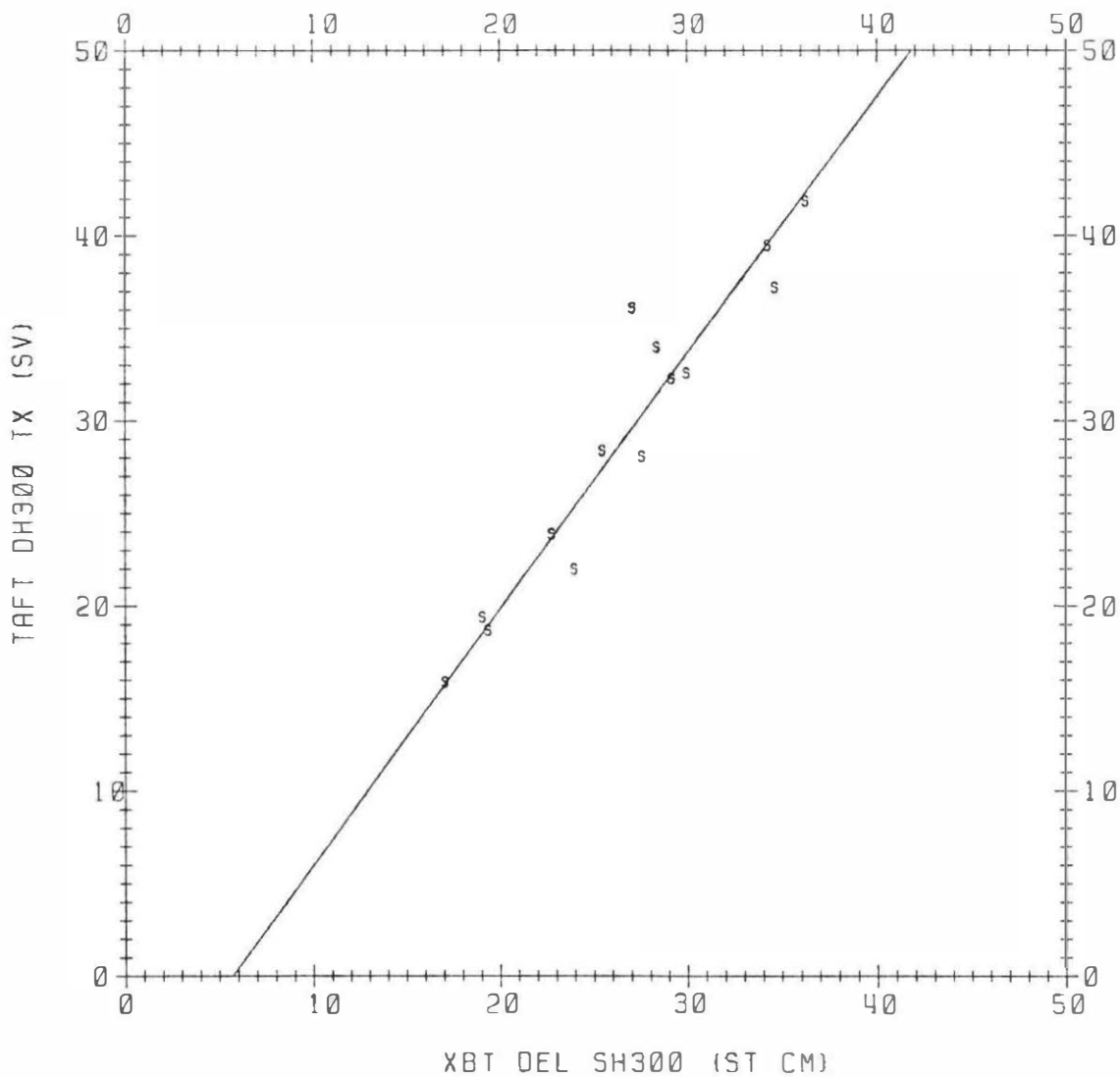
* POINTS = 42

R = 0.92

X-STDEAR = 12.5

Y-STDEAR = 2.6

Fig. 14. Comparison between the 2-Layer Approximation Method and Taft's calculations of geostrophic transport relative to 300 meters for the NECC.



SOUTH EQ. CURRENT

* POINTS = 14

R = 0.96

X-STDERR = 1.8

Y-STDERR = 2.5

Fig. 15. Comparing the steric height difference between the ridge and trough of the SEC with Taft's calculations of geostrophic transport relative to 300 meters for the SEC.

REFERENCES

- Barnett, T., and W. Patzert, Scales of Thermal Variability in the Tropical Ocean, *Journal of Physical Oceanography*, Vol. 10, no. 4, pp. 529-540, 1980.
- Cantos-Figuerola, A., and B. Taft, The South Equatorial Current during the 1979-80 Hawaii Tahiti Shuttle, *Tropical Ocean Atmosphere Newsletter*, no.19, July 1983.
- Firing, E., C. Fenander, and J. Miller, Profiling current meter measurements from the NORPAX Hawaii to Tahiti Shuttle Experiment, Univ. of Hawaii Ref. HIG 81-2, HIG data report no. 39, 146 pp., July 1981.
- Heinmiller, R. et al., Systematic errors in expendable bathythermograph (XBT) profiles, *Deep Sea Research*, vol. 30, no. 11a, pp. 1186-1197, 1983.
- Legeckis, R., Long waves in the eastern Equatorial Pacific Ocean: A view from a geostationary satellite, *Science*, vol. 197, pp. 1179-1181, 1977.
- Luther, D., Evidence of 4-6 day barotropic, planetary oscillation of the Pacific Ocean, *Journal of Physical Oceanography*, vol. 12, no. 7, pp. 644-657, July 1982.
- Meyers, G., and J. R. Donguy, The North Equatorial Counter Current and heat storage in the western Pacific during 1982-83, *Nature*, vol. 312, pp. 258-260, 1984.
- Molinari, R. et al., Subtropical Atlantic climate studies: Introduction, *Science*, vol. 227, pp. 292-311, Jan 1985.
- Montgomery, R. B., and E. D. Stroup, Equatorial Waters and Currents at 150 West in July-August 1952, *John Hopkins Oceanographic Studies*, no. 1, 68 pp., John Hopkins Press, Baltimore, Md., 1962.

Roemmich, D., Indirect sensing of Equatorial Currents by means of island pressure measurements, *Journal of Physical Oceanography*, vol. 14, pp. 1458-1469, Sept. 1984.

Taft, B., and P. Kovalala, Vertical sections of temperature, salinity, thermocline anomaly and zonal geostrophic velocity from NORPAX Shuttle Experiment, Part 1, NOAA Data Report ERL PMEL-3, 98 pp., July 1981.

Whitworth, T., Monitoring the transport of the Antarctic Circumpolar Current at Drake Passage, *Journal of Physical Oceanography*, vol. 13, pp. 2045-2057, Nov. 1983.

Wunsch, C., and A. Gill, Observations of equatorially trapped waves in Pacific sea level variations, *Deep Sea Research*, vol. 23, pp. 371-390, 1976.

Wyrтки, K. et al., The Hawaii to Tahiti Shuttle Experiment, *Science*, vol. 211, no. 4477, pp. 22-28.

Wyrтки, K., Eddies in the Pacific North Equatorial Current, *Journal of Physical Oceanography*, vol. 12, pp. 746-749, 1982.

Wyrтки, K., and R. Kendall, Transports of the Pacific Equatorial Counter Current, *Journal of Geophysical Research*, vol. 72, pp. 2073-2076, 1967.

Wyrтки, K., and B. Kilonsky, Transequatorial water structure during the Hawaii to Tahiti Shuttle Experiment, *Univ. of Hawaii Ref. HIG 82-5*, 65 pp., Aug. 1982.

Wyrтки, K., G. Meyers, D. Mclain, and W. Patzert, Variability of the thermal structure in the central Equatorial Pacific Ocean, *Univ. of Hawaii Ref. HIG 77-1*, 75 pp., January 1977.

Wyrтки, K., Monitoring the strength of the equatorial currents from XBT sections and sea level, *Journal of Geophysical Research*, vol. 83, no. C4, pp. 1935-1940, April 1978.